GEOSEA V Proceedings Vol. II, Geol. Soc. Malaysia, Bulletin 20, August 1986; pp. 701–762

Behaviour of tin and associated elements in a mountain stream, Bujang Melaka, Perak, Malaysia

W.K. FLETCHER[1], P.E. DOUSSET[1] AND YUSOFF BIN ISMAIL[2]
[1]SEATRAD Centre
[2]Geological Survey of Malaysia

Abstract: Results of geochemical drainage surveys for Sn are notoriously erratic and difficult to interpret. The object of this report is to examine some of the causes of these problems and suggest practical remedies.

The study area is a granitic dome, rising to 1242 m, on the eastern side of the Kinta Valley 33 km south-southeast of Ipoh, Malaysia. Drainage sediments and heavy mineral dulang concentrates were collected regionally at an average density of 1/km^2 and in much greater detail from a river, the Sungei Petai, draining known Sn mineralization. At each sampling site standard procedures for collecting active sediments were employed except that, wherever possible, separate samples were collected from high and low energy environments characterized by coarse- and medium- grained sands, respectively. After disaggregation and sieving, all samples were analysed for Sn, W, As, Cu, Pb, Zn and Fe. Magnetite content was also determined.

Tin, W and magnetite content of the sediments is strongly influenced by their hydraulic environment whereby significantly greater concentrations (up to twentyfold for Sn) are associated with high energy environments. As a result, enhanced Sn values are widely and erratically distributed on Bujang Melaka and provide an unreliable guide to exploration targets. In contrast, As, Cu, Pb and Zn, which are associated with the primary Sn mineralization, are not present in the sediments as heavy minerals and their concentrations, which are not perturbed by hydraulic conditions, are much less variable, These elements can therefore provide a more reliable guide to the source of Sn than Sn itself.

Detailed studies of the behaviour of Sn indicate that the Sungei Petai acts as a natural palung: light minerals are winnowed away leaving bedload sediments enriched in cassiterite. This process is most efficient for finer grain sizes and is significantly more effective in high, compared to low, energy environments except for the finest material. This difference is responsible for erratic within-site variations. Magnetite behaves in a hydraulically similar way to cassiterite, and the Sn/magnetite ratio can therefore be used to evaluate the significance of Sn concentrations. Thus, a high Sn content but low Sn/magnetite ratio probably reflects a hydraulic (placer) accumulation. Conversely, a high Sn content accompanied by a high Sn/magnetite ratio would indicate that Sn concentrations were more directly related to an anomalous source of Sn.

The concept of hydraulic equivalence of cassiterite and magnetite was extended to cassiterite and light minerals by determining (with an F-test) the size range of light minerals whose hydraulic behaviour is most similar to that of cassiterite grains having a different size. Minus 65+100 mesh was found to give the optimum results for all finer sizes of cassiterite so that plotting values of

$$\frac{Sn_x . W_x}{W_{-65+100}}$$

where Sn_x is the concentration of Sn in a size fraction, x, weight W_x and $W_{-65+100}$ is the weight of the minus 65+100-mesh fraction, minimise within-site variability and maximise anomaly contrast. Resulting geochemical patterns are then very similar to those for the pathfinder elements.

It is concluded that erratic distribution of Sn in drainage sediments reflects its variable enhancement in response to hydraulic conditions. Data interpretation can be improved using pathfinder elements, Sn/magnetite ratios or hydraulic equivalence concentrations of Sn. Use of minus 80-mesh material appears satisfactory for routine multi-element surveys, but where elements dispersed as heavy minerals are of especial interest, use of very fine (minus 270 mesh) sediment might be advantageous.

INTRODUCTION

Regional mineral exploration programmes are often based on or include reconnaissance geochemical drainage surveys and chemical or mineralogical analysis of heavy mineral pan (*dulang*[1]) concentrates—for example, Chand (1981). However, results of geochemical surveys for Sn and other elements, such as W and Au, dispersed as resistate heavy minerals, are notoriously erratic. Zantop and Nespereira (1979), for example, noted that sediment surveys gave many one-spot anomalies and attributed their erratic results to: (a) variations in cassiterite grain size, (b) considerable variability—up to tenfold—encountered at each sampling site, and (c)subsampling errors in sample preparation and analysis. Similarly, Kaewbaidhoon (1961), working in the present study area, observed that Sn content of anomalous sediments was very susceptible to environmental effects, as concentrations consistently increase with increasing stream velocity. Furthermore, as reported by Hosking *et al.* (1962), it is not unusual for maximum Sn concentrations in drainage sediments to be considerably displaced from their source.

As a result of the foregoing problems, some workers (e.g., Zantop and Nespereira, 1979) have discarded geochemical data for Sn in sediments and recommend visual estimation of cassiterite content of pan concentrates after bromoform flotation. However, in so far as multi-element reconnaissance geochemical surveys are very widely utilized, it seems desirable to maximise the amount of information gained providing this can be done without greatly increasing costs. Furthermore, at a practical level, seasonal lack of surface water can prelude on-site panning in some regions.

Providing subsampling and analytical problems are overcome, the principal difficulty in interpreting geochemical drainage data for Sn arises, as outlined above, from its erratic distribution pattern. As reported for barium by Sleath and Fletcher (1982), this is a characteristic of the behaviour of elements present in drainage sediments as resistate heavy minerals that results from differential winnowing, sorting and accumulation of light and heavy mineral grains in response to changing hydraulic conditions during transport. Unfortunately, although general conditions favouring accumulation of heavy minerals at a site are well known (and are routinely taken advantage of in producing a pan concentrate), the theoretical behaviour of particles moving in an aqueous flow system is extremely complex and cannot be reliably predicted.

Empirical studies of the relative behaviour of light and heavy minerals in fluviatile sediments made by Rittenhouse (1943) led to the concept of hydraulic equivalence (i.e., those grains of different minerals that—although of different size—have the same sedimentological behaviour). However, with the notable exception of Gladwell's (1981) study of behaviour of Sn in drainage sediments from southwest England, there have been no systematic attempts to correct Sn concentrations in drainage sediments for hydraulic conditions.

---

[1] a shallow wooden bowl used in Malaysia for panning heavy mineral concentrates

The following study has therefore been undertaken of the behaviour of Sn in the mountain streams where Kaewbaidhoon (1961) observed severe hydraulic environmental effects on Sn content of anomalous sediments.

Objectives were:

(1) to provide an orientation survey of the dispersion of tin and associated pathfinders in soils and sediments; and
(2) to develop improved methods of interpretation of geochemical drainage data for Sn.

DESCRIPTION OF STUDY AREA

Location and access

Gunung Bujang Melaka, a satellite granitic dome of the Main Range Batholith, is located approximately thirty-three kilometres south-southeast of Ipoh and east of the town of Kampar, Perak (Figure 1). Detailed studies were undertaken on the Sungei Petai located on the western side of Bujang Melaka immediately north of Kampar. Paved roads around the dome provide relatively easy access to its lower slopes. Access to its interior, however, requires foot traverses in steep jungle terrain occasionally facilitated by logging roads of very variable condition.

Geology

Geology of Bujang Melaka has been described by Ingham and Bradford (1960). The main granite is medium grained, contains biotite and is often coarsely porphyritic. This is cut by finer grained biotite granites with abundant tourmaline. Age dating and isotopic studies (Bignell and Snelling, 1977) give concordant K:Ar and Rb:Sr dates of 211 ± 5Ma. The value (0.7165 ± 0.0009) of the $^{87}Sr:^{86}Sr$ ratio was higher than that for any other Malaysian granite they studied and suggests that anatectic melting of sialic crust played an important role in magma generation.

Previous geochemical studies (Kaewbaidhoon, 1961) clearly indicate the stanniferous character of Bujang Melaka compared to adjoining parts of the Main Range. Further evidence of its tin-rich character is found in the alluvial tin deposits of the surrounding valleys. However, (legal) mining of tin on Bujang Melaka has been limited to mining (that ceased in 1929) of primary mineralization from ore bodies associated with pegmatite pipes and aplites at Ulu Petai (Ingham and Bradford, 1960). In addition to cassiterite, the following were noted: topaz, fluorite, tourmaline, pyrite, chalcopyrite and wolframite. Riley (1968) also identified arsenopyrite, galena, sphalerite and sulphosalts in dump material. Cassiterite is the only tin mineral observed in pan concentrates.

Topography, sediments, climate, soils and vegetation

The Bujang Melaka granite forms a large elliptical dome-shaped mass rising steeply, from the Kinta Valley (approximately 30 m above sea level at Kampar) on the west and from the deeply incised Sungei Chenderiang on the east, to its maximum elevation of 1242 m. Subsidiary peaks lie N-S along the principal axis of the ellipse. Drainage is radial and weakly dendritic with swift, deeply incised mountain streams. Stream waters are usually clear (except downstream of logging roads after heavy rain) and moderately acidic (pH $\simeq$ 5).

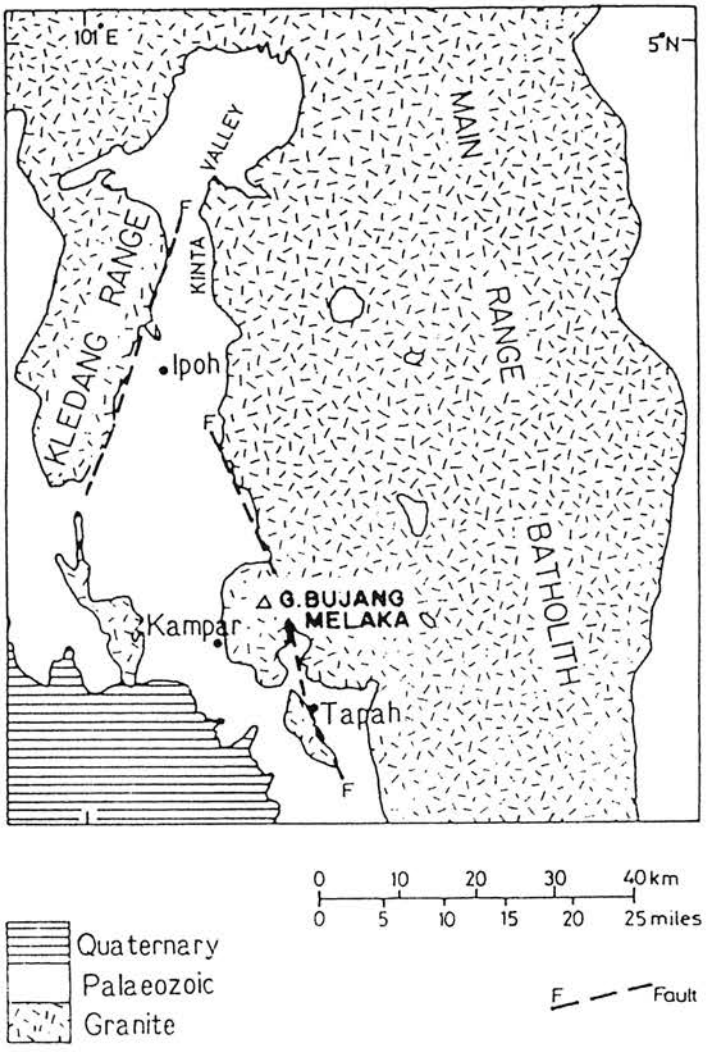

Fig. 1 Location of study area. Modified from Bignell and Snelling (1977).

The Sungei Petai, the focus of detailed studies, is a typical stream. It has an average gradient approaching 1:4 and for a large proportion of its course the stream either flows over outcrops of granite with numerous waterfalls or beneath large granitic core boulders where it is inaccessible (Figure 2). As a result, suitable sampling sites can be difficult to find. At sample sites in the middle and lower reaches of the stream, high and low energy environments characterized by moderately sorted, very coarse sandy gravel and medium-grained sands, respectively, were visually identified. Above 550 m (Station 19) no such distinction can be made. Longitudinal profiles of sediment texture show an increase in medium (minus 65+100 mesh) sand content, with a concomitant decrease of coarse (minus 28+35 mesh) sand below this point (Figure 3). Coarse sand content increases again downstream from Station 10.

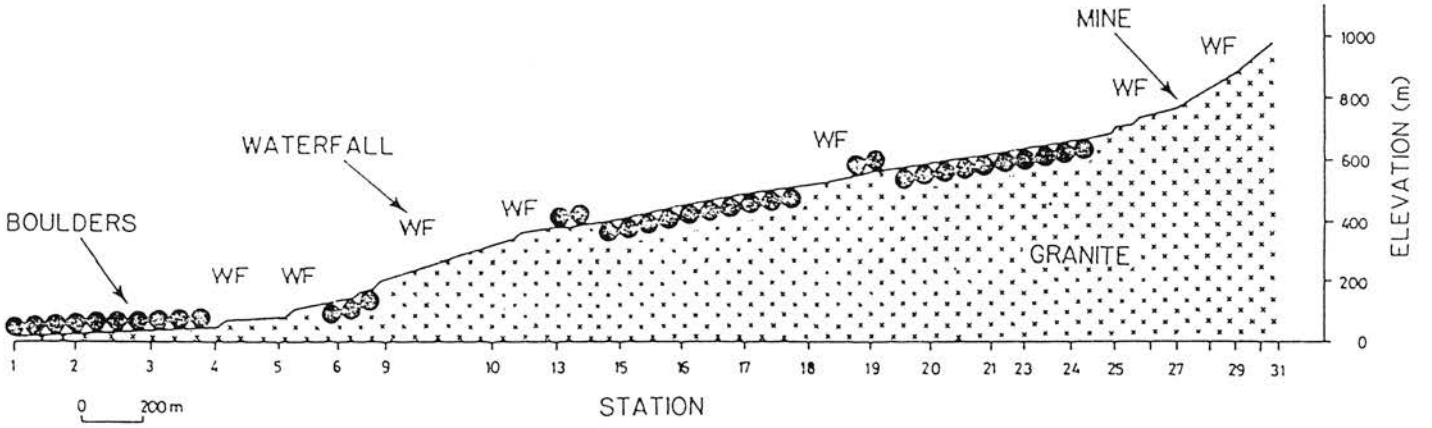

Fig. 2 Longitudinal profile of Sungei Petai.

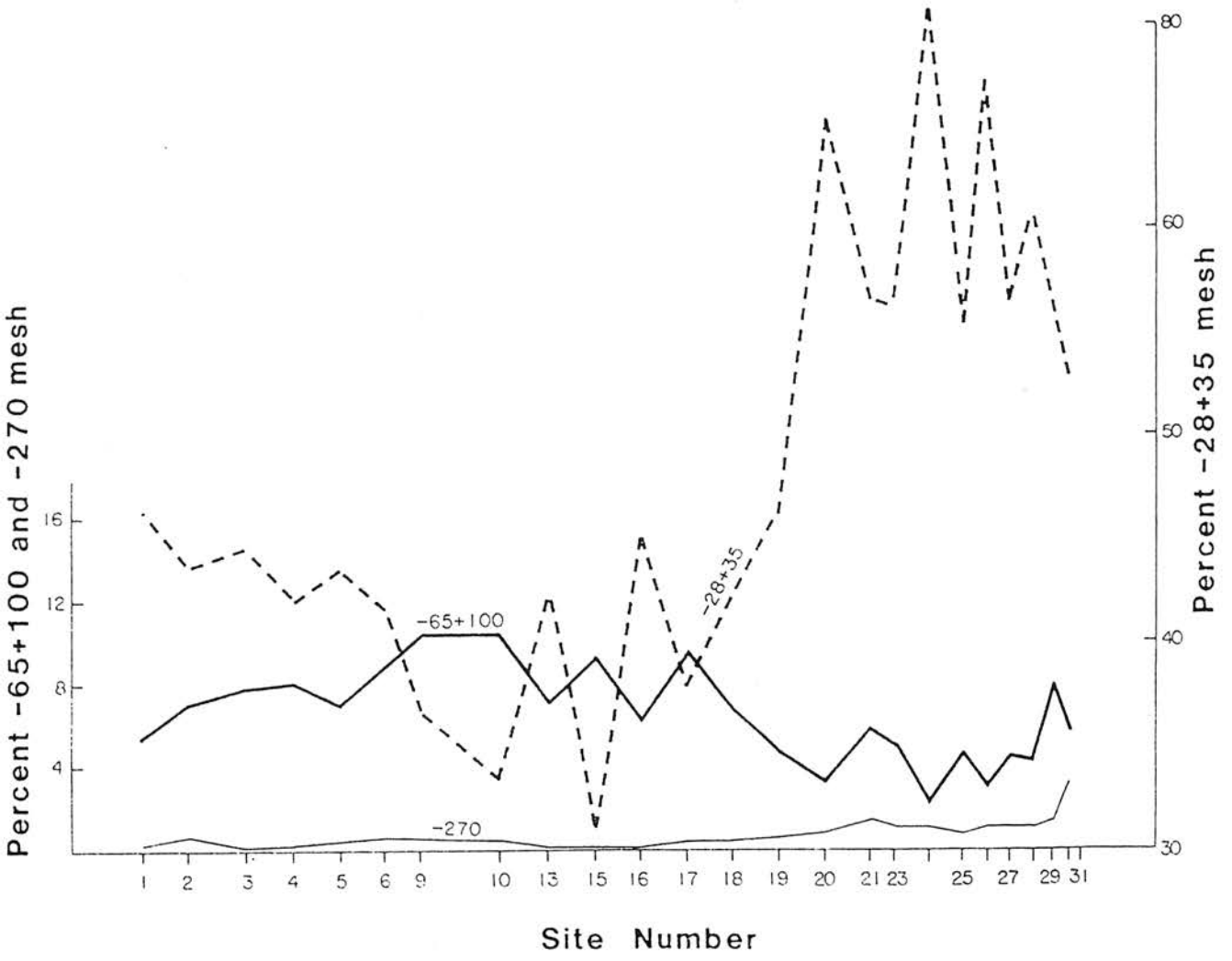

Fig. 3 Variations in sediment texture in the Sungei Petai.

Rainfall at Kampar averages 363 cm per year, and up to 19 cm has been recorded in a 24-hour period (Ingham and Bradford, 1960). Rainfall at higher elevations on Bujang Melaka, which is frequently hidden in cloud, is probably even higher. The average annual temperature for the floor of the Kinta Valley at Kampar is 28°C (82°F) with little diurnal or annual variation.

Steep slopes have limited land clearance on Bujang Melaka, and it is largely covered by primary Dipterocarp jungle. Soils have not been studied extensively. However, at Ulu Petai (940 m), where detailed soil geochemical studies were undertaken, it is apparent that steep slopes generally prevent development of mature profiles. Nevertheless, leaching is severe and can lead to development of a sandy, bleached Ae horizon on gentler slopes (Table 1). Acid brown forest soils and podzols are therefore probably typical of these elevations.

METHODS

Sampling

Sediments

To establish metal distributions and background concentrations, active drainage sediments were collected from most of the streams draining Bujang Melaka (Figure 4). Two samples of sediment were collected at each location: one of relatively coarse sediment from a high energy environment and another of relatively finer, medium-grained sand from a low energy environment. Sediments of the latter type were often impossible to obtain in stream headwaters; in this case, duplicate samples of coarse sediments were taken a few metres apart. In addition to sediment, a heavy mineral concentrate was collected using a half standard *dulang* to pan very coarse sediment.

Detailed studies on the Sungei Petai involved similar procedures. However, in addition to normal size geochemical samples, bulk sediment samples—weighing up to 10 kg—were

TABLE 1
SOIL PROFILE DESCRIPTION AND ANALYSIS, SITE 10 AT 936 M BUJANG MELAKA: SLOPE 15°

Depth (cm)	pH	% <53 μm	Description
0-4	5.2	3	Black-brown,soft,friable with abundant roots, no stones
4-19	5.5	7	Grey-brown, very sandy, granular and very friable
19-28	5.4	10	Dark-brown, very sandy clay, compact, few roots, no stones
28-36	5.4	13	Yellow ferruginous sandy clay with 2mm Fe-oxide layer at top. No primary structure
36-46	5.3	15	As above but more pallid becoming white-pale grey at base
46-56	5.4	18	White-pale grey sandy clay
56-66	5.3	16	White-pale grey sandy clay
66-120	5.4	12	White, friable with bedrock (granite) structure

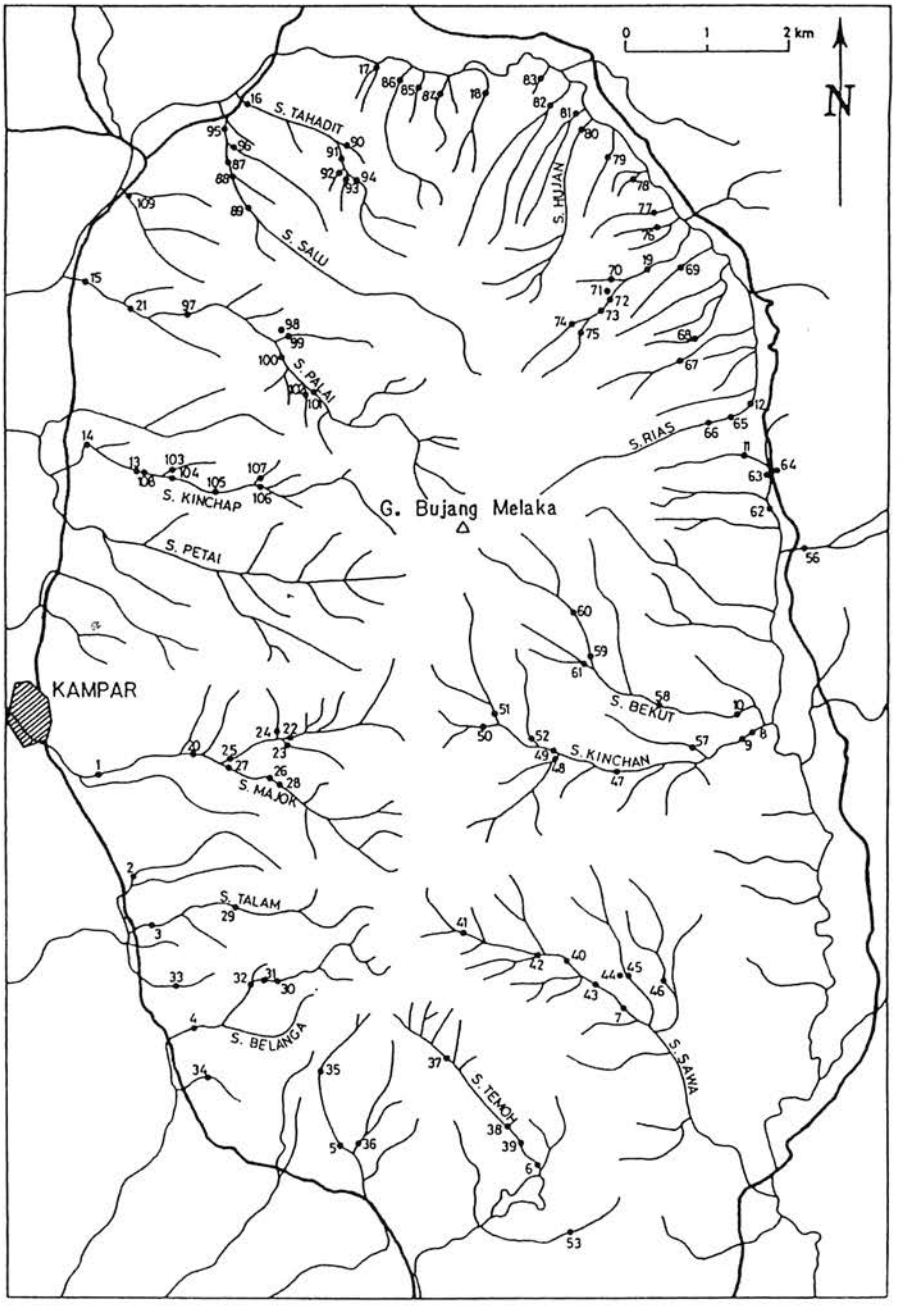

Fig. 4 Regional sediment sampling locations.

taken from high and low energy environments at stations approximately 200 m apart (Figure 5). Heavy mineral concentrates were also collected.

Sample preparation

Sediments

Standard size sediment samples were oven dried in their paper bags, disaggregated with a porcelain mortar and pestle and dry sieved through 80-mesh (177μm) nylon screen. The minus 80-mesh fraction was then analyzed without grinding. For size fraction analysis, bulk samples of sediments were air dried on large trays, disaggregated and dry sieved through nested stainless steel sieves on an Endecotts Test Sieve Shaker. Sieved fractions were weighed and then split and pulverized in a ring mill. To minimize sampling errors, the quantity of material pulverized was increased with increasing grain size to a maximum of 400 g (Table 2).

Magnetite separates

Depending on availability of material, magnetite was separated from sediments in two ways. When sample size was not a limiting factor, the sample was fed through a Carpco induced roll lift-type magnetic separator. However, in the case of the minus 80-mesh sediments the amount of material was usually insufficient for this procedure to be used. These samples were therefore suspended in water with a rotating paddle and magnetite collected by a small bar magnet inserted in a glass tube and immersed in the suspension. Magnetite attracted to the tube was washed off, collected on filter paper, air dried and weighed.

Heavy mineral concentrates

Heavy mineral concentrates were examined mineralogically by the Geological Survey of Malaysia, using their routine procedures, and also at SEATRAD Centre. Pulverized splits were prepared for determination of Sn by chemical analysis.

TABLE 2
TYPICAL WEIGHT OF VARIOUS SIZE FRACTIONS GROUND TO MINUS 200 MESH PRIOR TO ANALYSIS

Size fraction		
Mesh	μm	Weight (g)
– 270	< 53	5
– 200 + 270	75 – 53	5
– 150 + 200	106 – 75	5
– 100 + 150	150 – 106	20
– 65 + 100	212 – 150	50
– 48 + 65	300 – 212	200
– 35 + 48	425 – 300	400
– 28 + 35	600 – 425	400
– 20 + 28	850 – 600	400

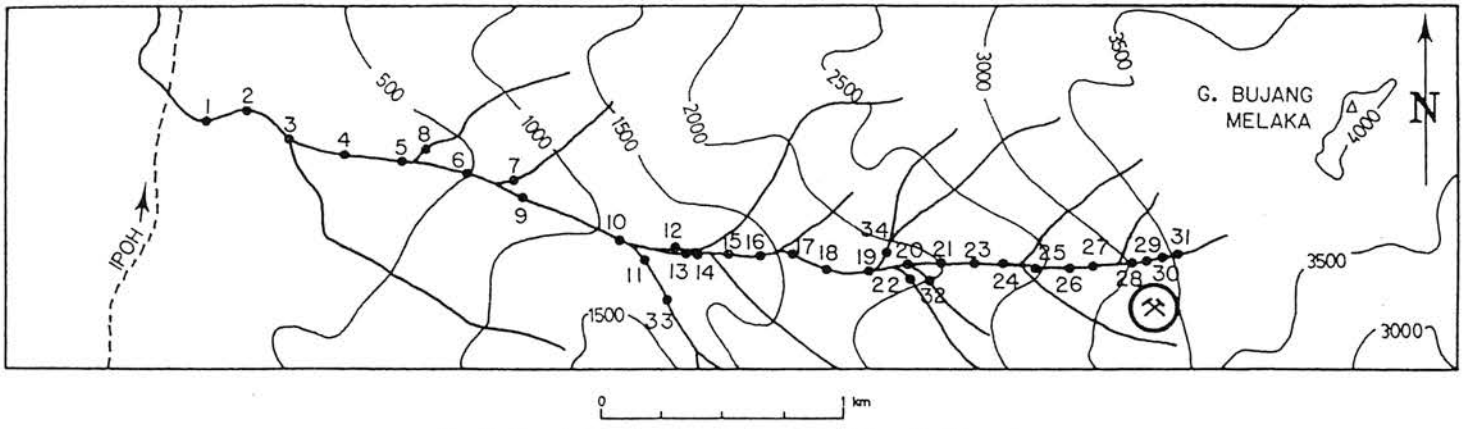

Fig. 5 Sample locations along the Sungei Petai (see also Figure 4).

TABLE 3
ANALYTICAL METHODS

Element	Method
Sn	NH_4I fusion: gallein colorimetry
As	potassium hydrogen sulphate fusion-colorimetry with Gutzeit test
W	potassium hydrogen sulphate fusion-colorimetry with zinc dithiol
Cu, Pb Zn, Fe	digestion with 3:1 50% HCl-HNO_3 followed by atomic absorption with background correction for Pb

Analysis

All samples were analysed by the rapid analytical procedures, routinely employed for geochemical samples at SEATRAD Centre, summarized in Table 3. Analytical precision (at the 95% confidence level) based on random duplicate pairs (Fletcher, 1981) was better than ± 40 percent for Sn on pulverized sieve fractions of drainage sediments.

STREAM SEDIMENT GEOCHEMISTRY OF BUJANG MELAKA

Regional studies were confined to analysis of stream sediments and heavy mineral concentrates collected from streams on Bujang Melaka. Standard sampling, sample preparation and analytical procedures were used both to collect the heavy mineral concentrate and active sediment, except that in the case of the latter one high energy (coarse sand) and one low energy (medium sand) sample were taken at each site. The objectives of this phase of the study were twofold: (i) to determine typical metal concentrations and geochemical patterns associated with the Bujang Melaka granite, and (ii) to illustrate any interpretative problems that might arise with geochemical data obtained by routine procedures.

Results

Analytical results for regional stream sediments are summarized in Table 4. The stanniferous character of Bujang Melaka, and to a lesser extent its enrichment in W and As, is immediately evident. Furthermore, concentrations of Sn, W, and As all span concentration ranges of one to two orders of magnitude. Abundances of the remaining elements (Cu, Pb, Zn and Fe) are not unusual for granitic terrains, and the range of concentrations for Cu, Pb and Zn is relatively narrow.

The second striking feature of the data is the contrast between Sn and magnetite contents of high versus low energy sites, with the former averaging a twofold enhancement. In the case of Sn, differences at individual sites can exceed 20x. The same phenomenon is shown, to a lesser extent, by W but not by any of the remaining elements.

Probability plots (Sinclair, 1976) have been used to partition the data and results, summarized in Table 5, used as a basis for defining class intervals in construction of geochemical maps. In all cases the populations approximated lognormality. When only one population was present, it was subdivided on the basis of its mean ($\bar{x}$) and standard

TABLE 4
REGIONAL STREAM SEDIMENT DATA MINUS 80-MESH FRACTION, BUJANG MELAKA
(All results in ppm unless otherwise specified)

Analysis	Stream environment	
	High energy	Low energy
Magnetite	1991[1] 46-871[2]	83 14-506
Sn	424 38-4764	174 24-1273
W	43 7-269	31 6-165
As	21 2-195	23 4-141
Cu	6 3-13	5 2-11
Pb	21 12-38	19 9-43
Zn	24 10-58	23 8-62
Fe(%)	1.12 0.41-3.06	1.08 0.36-3.27
Sn/magnetite	1.98 0.30-13.23	1.77 0.32-9.74

1 Geometric mean ($\bar{x}$)
2 $\bar{x} \pm 2s$ s = Log standard deviation

deviation(s) to give classes: $< \bar{x} - 2s$; $\bar{x} - 2s$ to $\bar{x} - s$; $\bar{x} - s$ to $\bar{x} + s$; $\bar{x} + s$ to $\bar{x} + 2s$; and $> \bar{x} + 2s$. For multimodal data, class intervals were selected to optimise separation of populations.

Resulting geochemical maps indicate that despite the large concentration ranges of Sn and W, their regional distributions do not show strongly defined geochemical patterns or trends. However, there are minor exceptions to this:

(1) Tin (Figures 6 and 7): the relative abundance of values exceeding $\bar{x} + s$, particularly for low energy samples, in the Sungei Palai and Sungei Kinchap, on the western flank of Bujang Melaka, and in one stream in the northeast.
(2) Tungsten (Figures 8 and 9): a cluster of above-average values in the headwaters of the Sungei Kinchan and Sungei Bekut.

Like Sn and W, drainage sediments on Bujang Melaka are characterised by a wide range of relatively high As concentrations (Figures 10 and 11). However, unlike Sn and W, distribution of As shows distinct trends with two clusters of values exceeding 65 ppm ($\bar{x} +$ s for high energy environments): one cluster in the Sungei Talam and Sungei Belanga and

TABLE 5
POPULATION PARAMETERS DERIVED FROM PROBABILITY PLOTS FOR REGIONAL STREAM SEDIMENT DATA, BUJANG MELAKA

Element / Environment	N	Estimated parameters (ppm)					
		P%[1]	$\bar{x} - 2s$[2]	$\bar{x} - s$	$\bar{x}$	$\bar{x} + s$	$\bar{x} + 2s$
Sn_H[3]	145	100	35	120	420	1450	5000
Sn_L[3]	78	100	16	50	160	520	1680
W_H	123	100	9	17	44	115	300
W_L	54	100	6	14	32	72	170
As_H	123	100	2	6	20	65	205
As_L	54	100	3	9	24	66	180
Cu_H	119	100	4	5	6	9	12
Cu_L	53	100	3	4	6	8	12
Pb_H	119	100	13	17	22	29	38
Pb_L	53	35	18	23	31	41	55
		65	7	12	14	18	22
Zn_H	119	30	21	24	28	32	37
		70	9	14	23	37	60
Zn_L	53	100	10	14	22	35	55
Fe_H(%)	119	80	0.7	1.0	1.4	2.0	2.8
		20	0.3	0.4	0.5	0.7	0.8
Fe_L(%)	53	100	0.4	0.7	1.1	1.9	3.3

[1] Proportion of total population

[2] $\bar{x}$ Log mean and (s) standard deviation

[3] H = High energy environment L = Low energy environment

the other in the Sungei Palai and Sungei Kinchap. The latter cluster corresponds to a zone of enhanced Sn values. A zone of relatively low As concentrations, with many values less than 6 ppm, characterises the NE side of Bujang Melaka.

For the remaining elements, the most notable regional features are (i) relative abundance of above average and regionally anomalous Cu concentrations (Figures 12 and 13) in the Sungei Palai and Sungei Kinchap— coinciding with the Sn and As anomalies already noted; and (ii) relative depletion of Zn (Figures 14 and 15) and Fe (Figures 16 and 17) in the Sungei Kinchan and Sungei Majok catchments. Variations in distribution of Pb are within the range of analytical error and probably not significant.

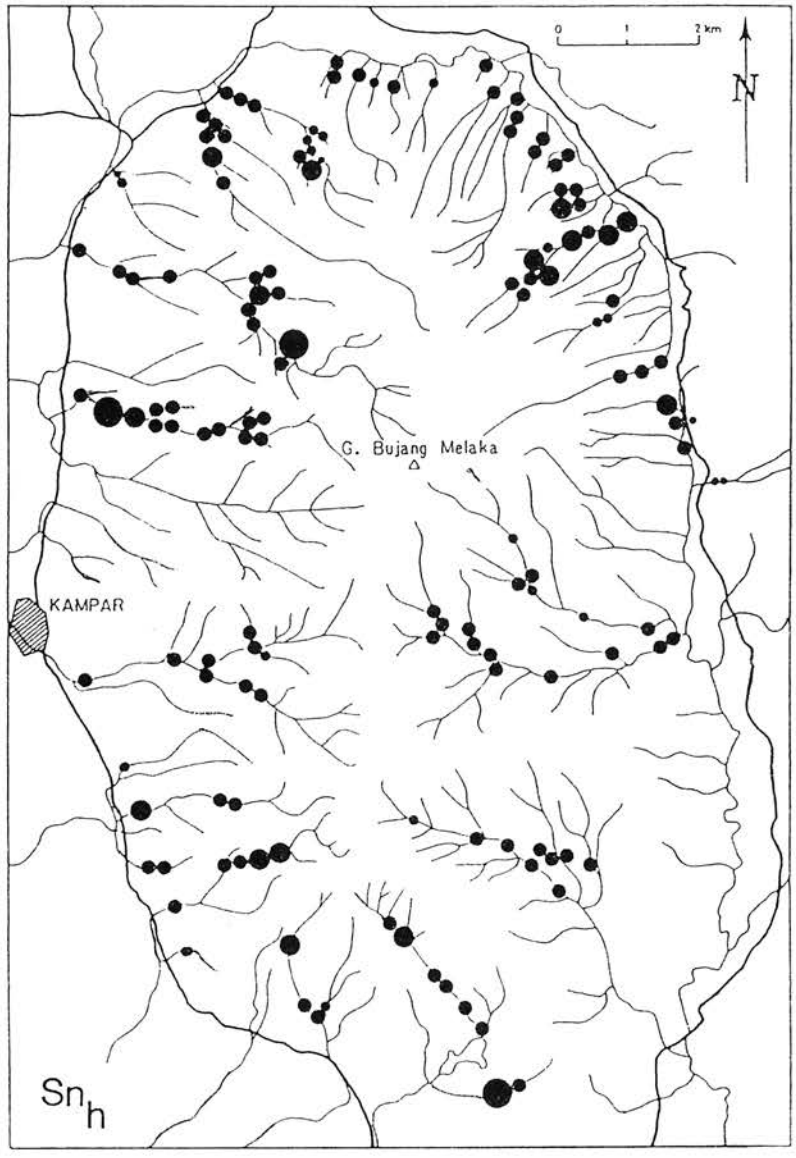

KEY TO SYMBOLS

	ppm
$\bar{x}+2s$	5000
$\bar{x}+s$	1450
$\bar{x}-s$	120
$\bar{x}-2s$	35

Fig. 6 Distribution of Sn in minus 80-mesh fraction, high energy environments.

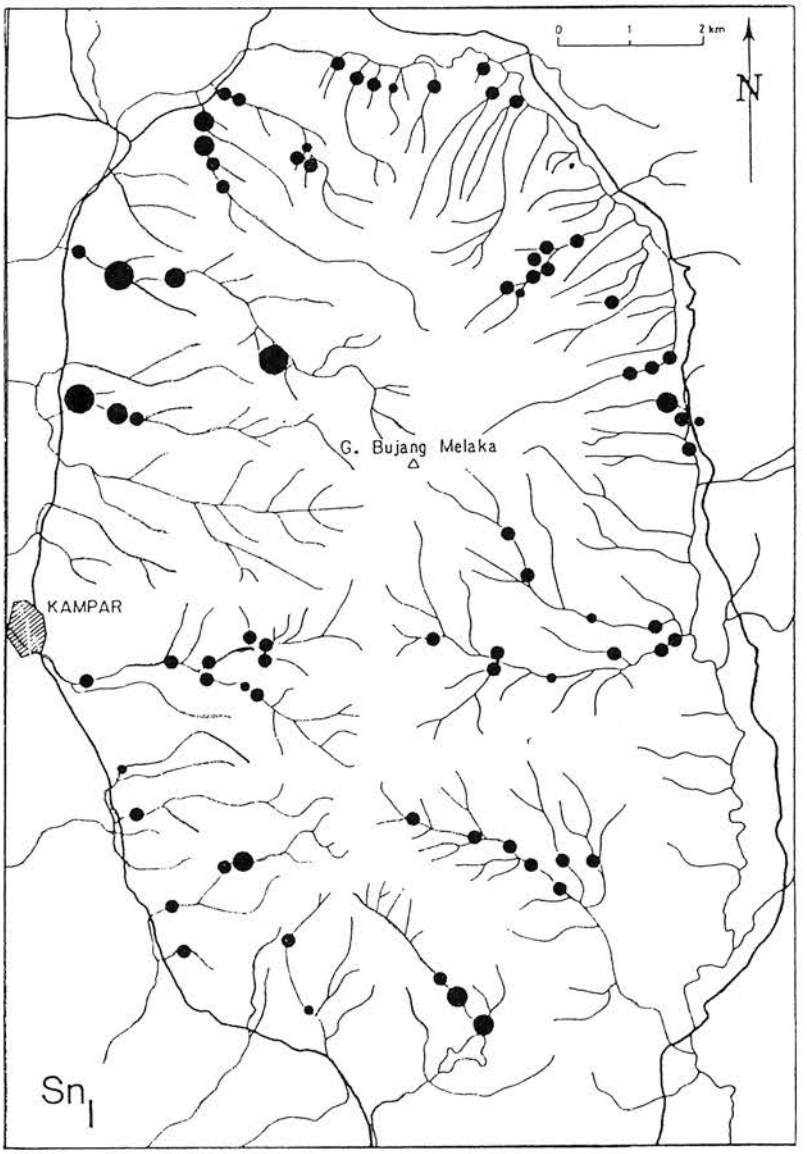

Fig. 7 Distribution of Sn in minus 80-mesh fraction, low energy environments.

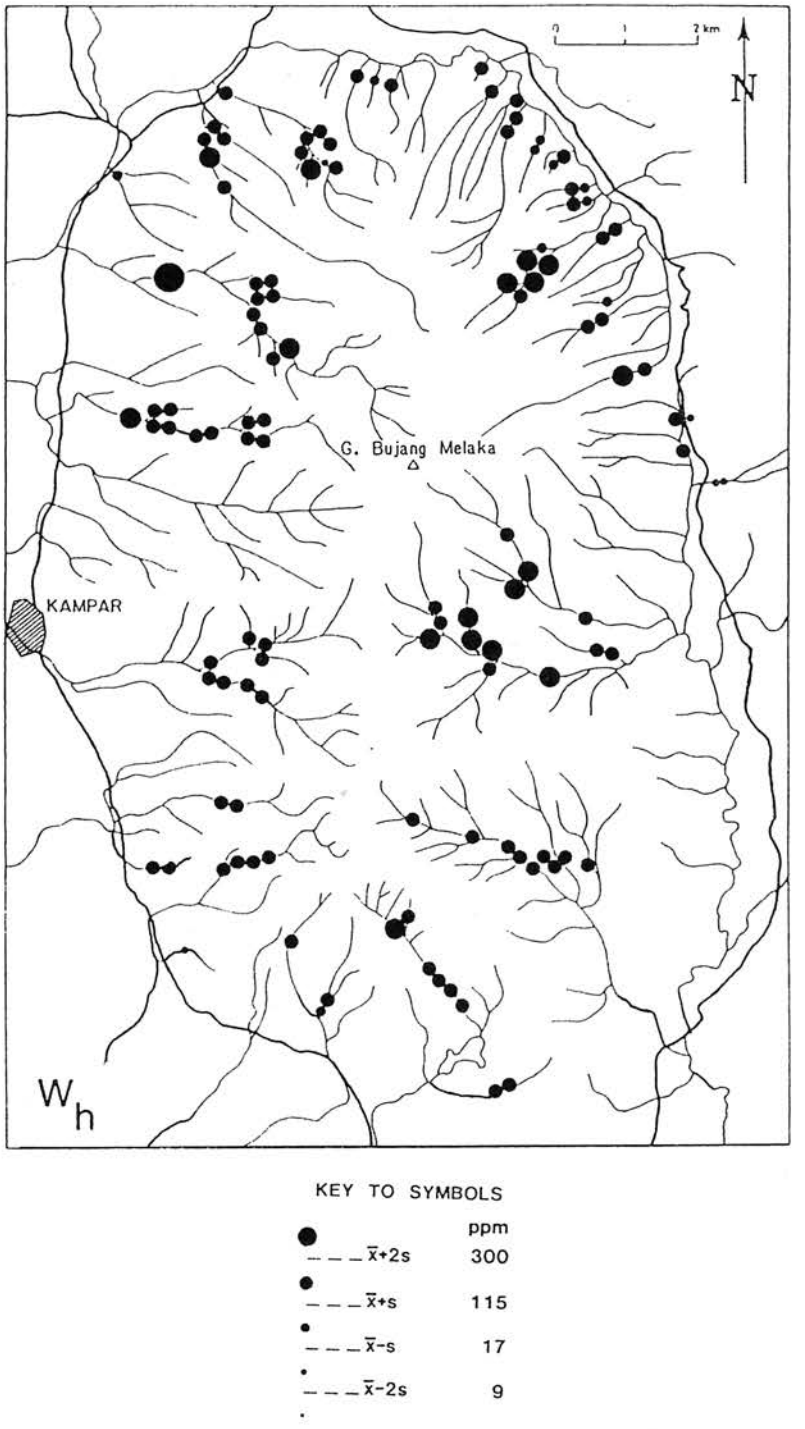

Fig. 8 Distribution of W in minus 80-mesh fraction, high energy environments.

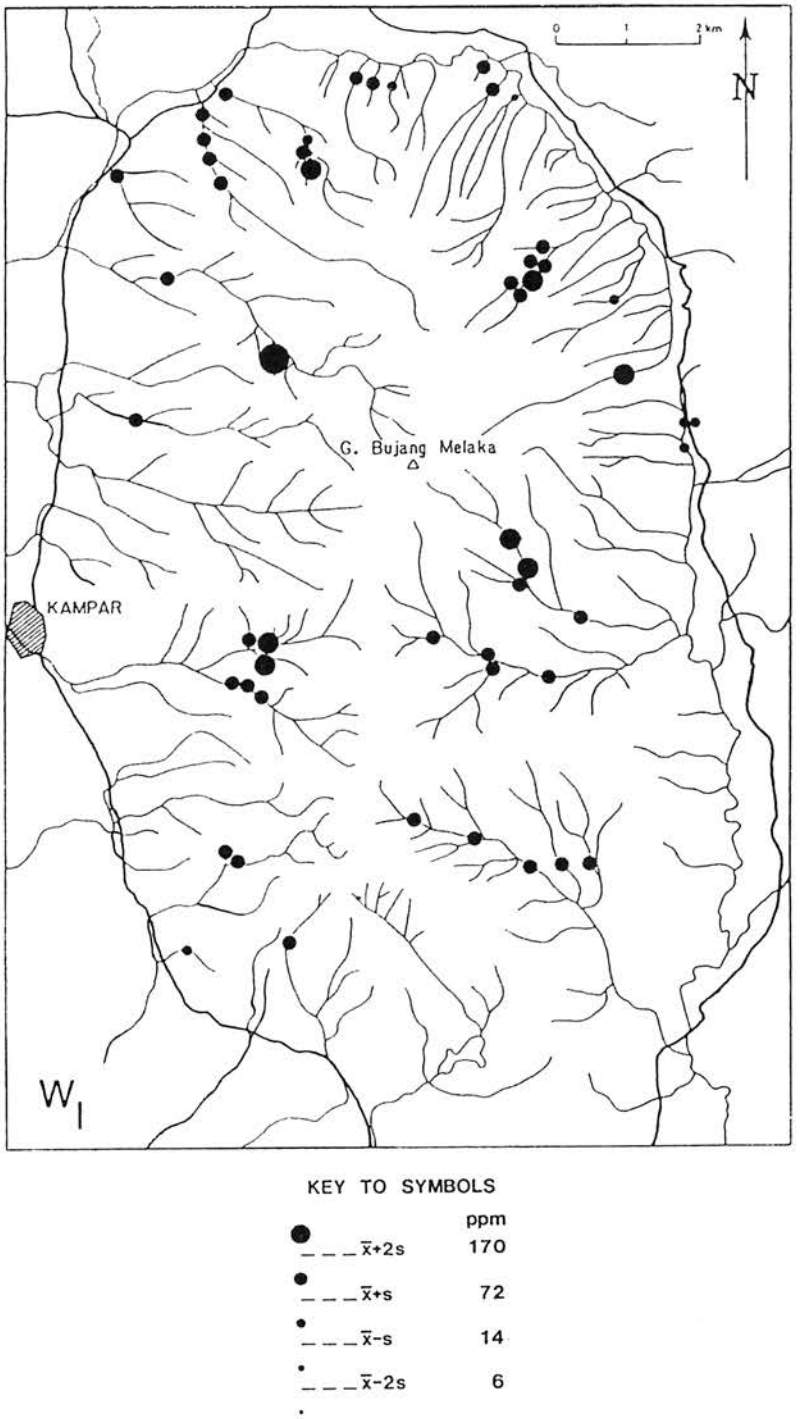

Fig. 9 Distribution of W in minus 80-mesh fraction, low energy environments.

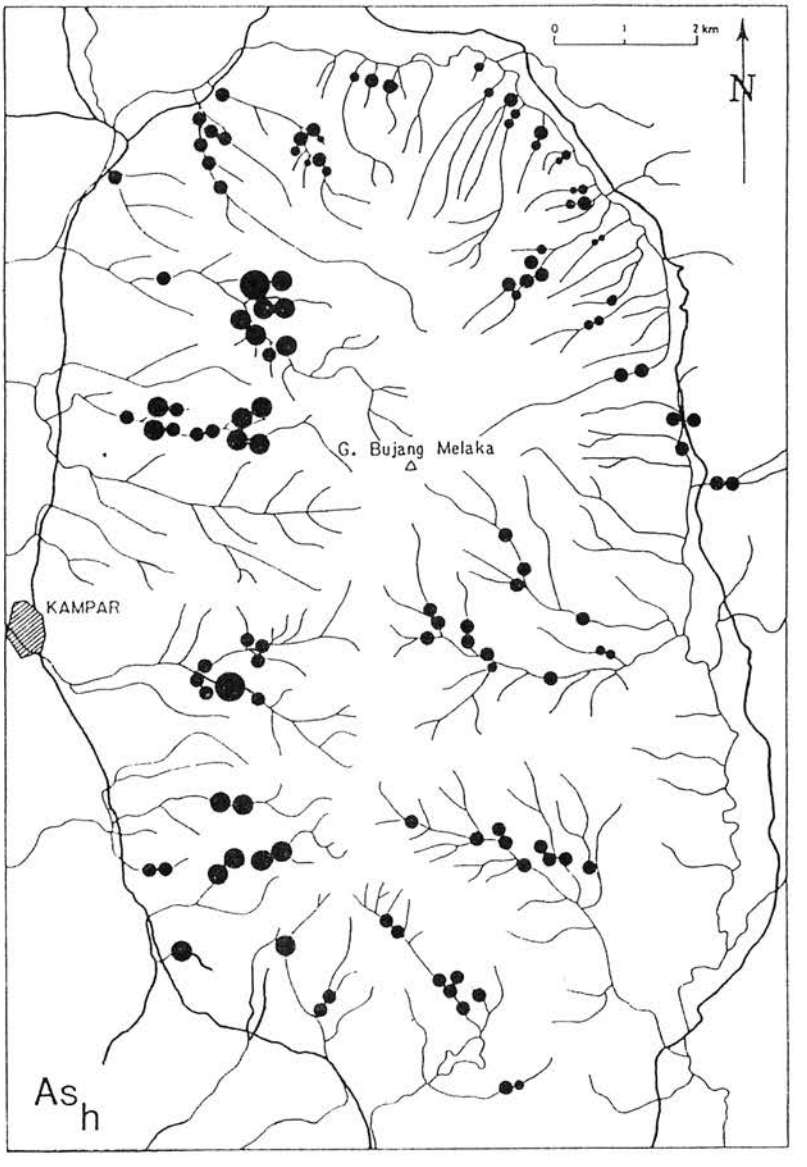

Fig. 10 Distribution of As in minus 80-mesh fraction, high energy environments.

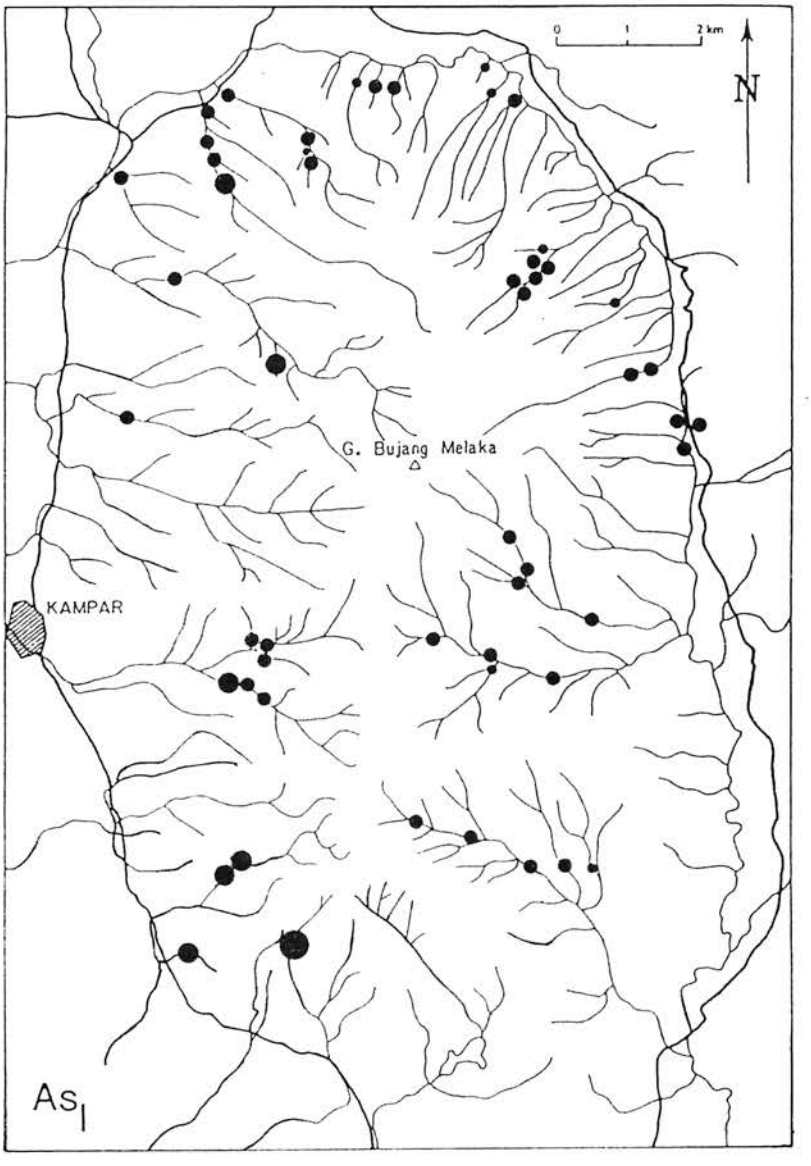

KEY TO SYMBOLS

	ppm
$\bar{x}+2s$	180
$\bar{x}+s$	66
$\bar{x}-s$	9
$\bar{x}-2s$	3

Fig. 11 Distribution of As in minus 80-mesh fraction, low energy environments.

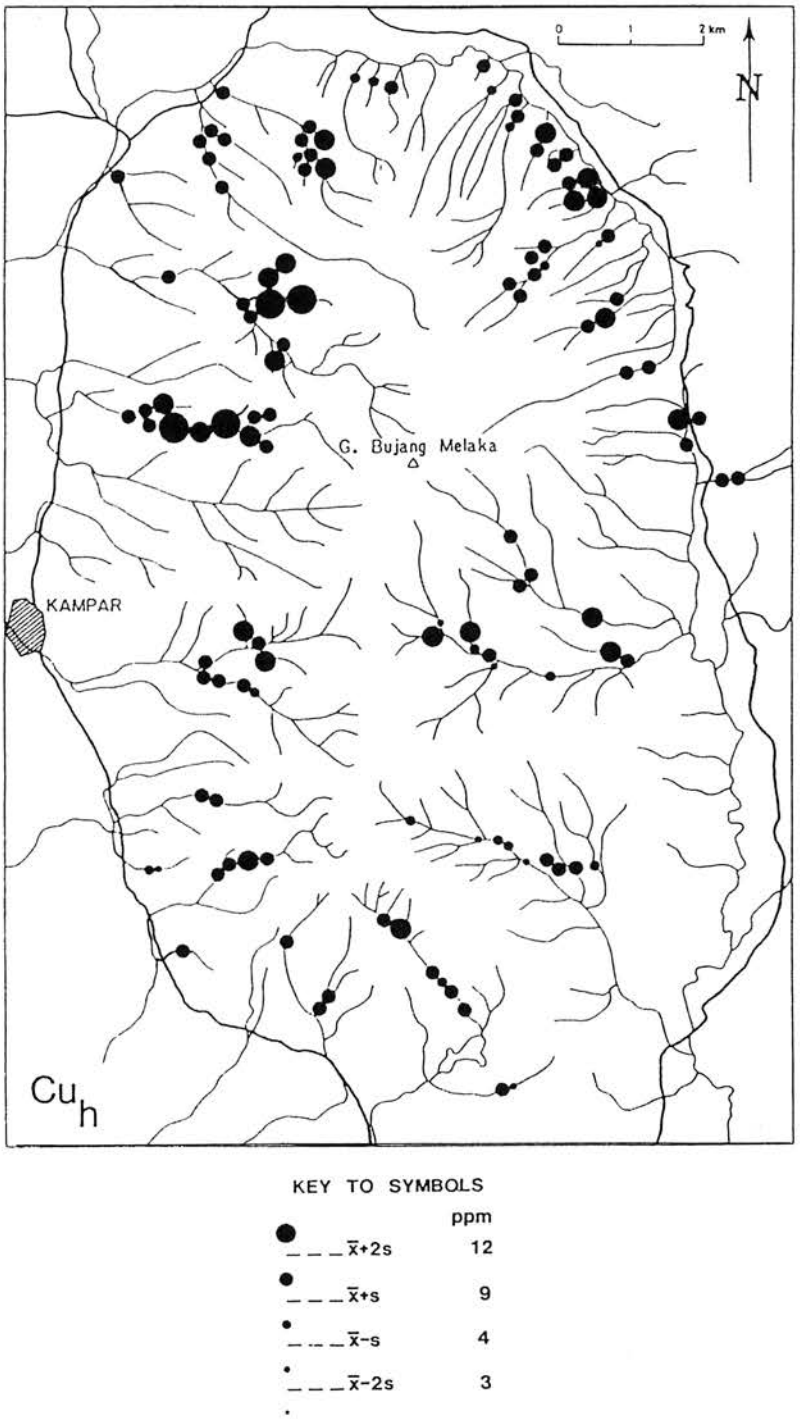

Fig. 12 Distribution of Cu in minus 80-mesh fraction, high energy environments.

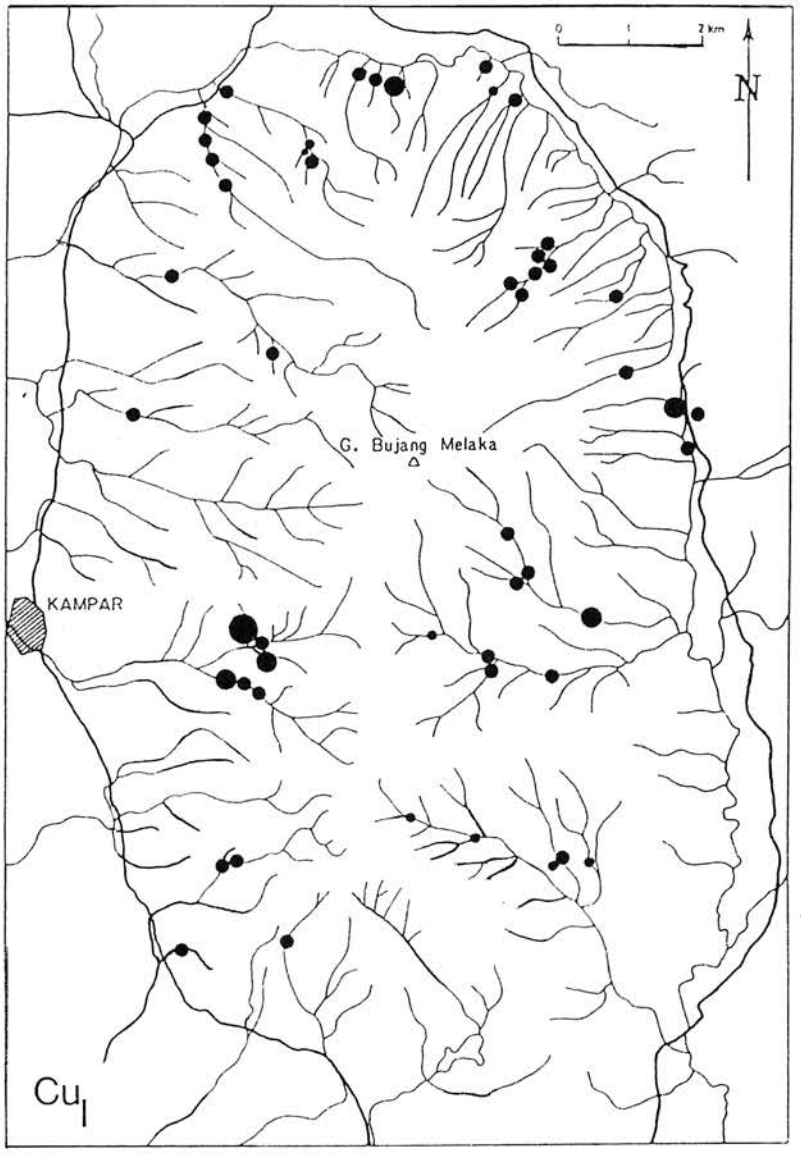

KEY TO SYMBOLS

	ppm
$\bar{x}+2s$	12
$\bar{x}+s$	8
$\bar{x}-s$	4
$\bar{x}-2s$	3

Fig. 13 Distribution of Cu in minus 80-mesh fraction, low energy environments.

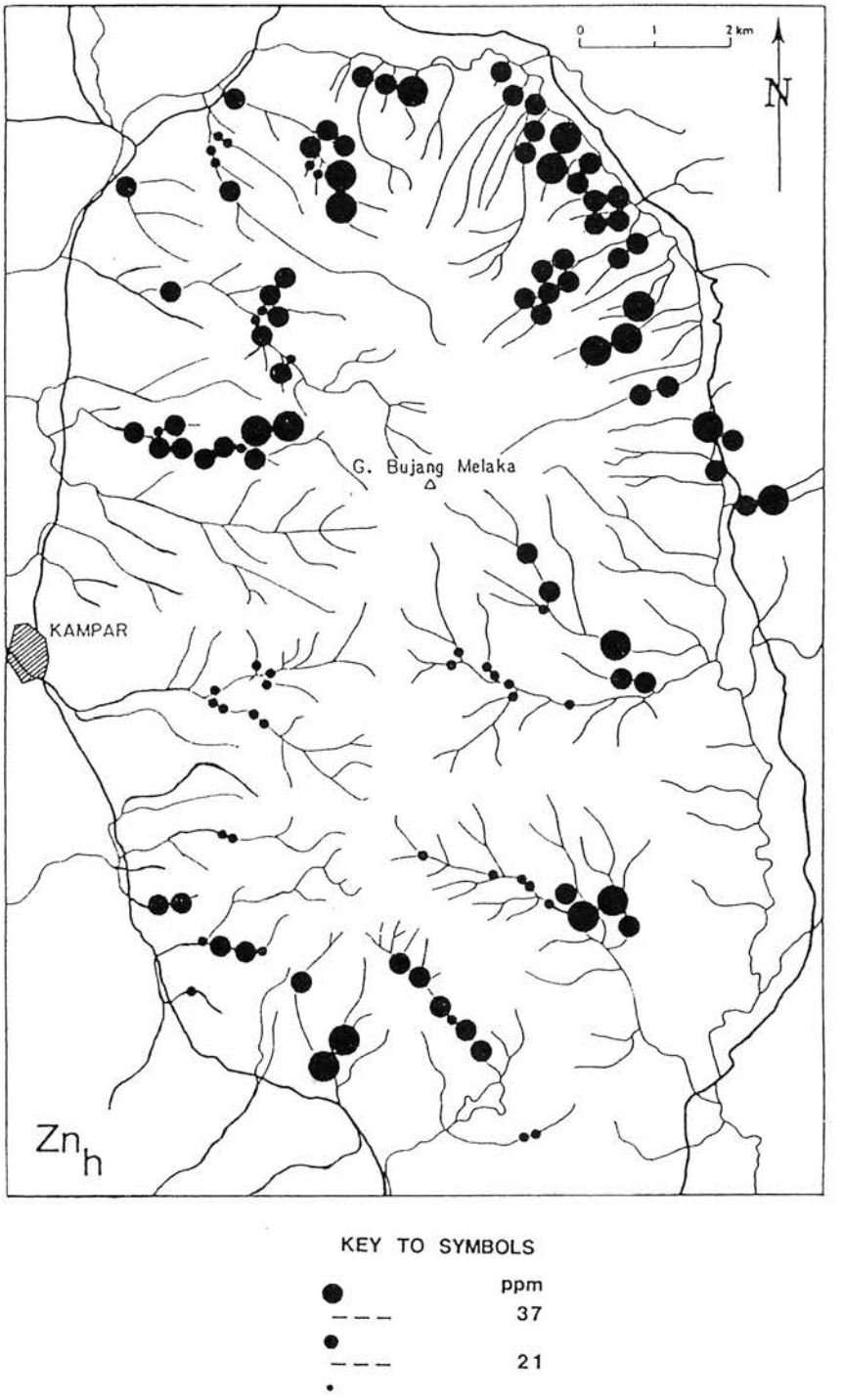

Fig. 14 Distribution of Zn in minus 80-mesh fraction, high energy environments.

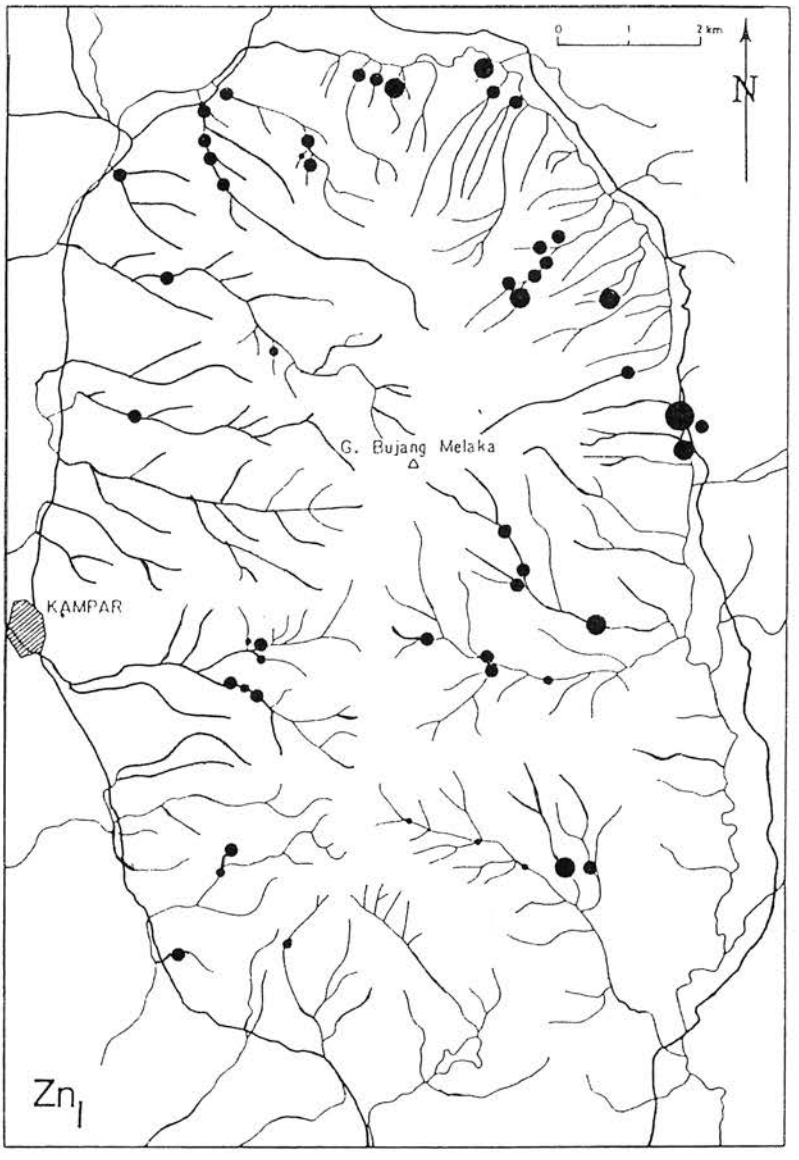

KEY TO SYMBOLS

	ppm
$\bar{x}+2s$	55
$\bar{x}+s$	35
$\bar{x}-s$	14
$\bar{x}-2s$	10

Fig. 15 Distribution of Zn in minus 80-mesh fraction, low energy environments.

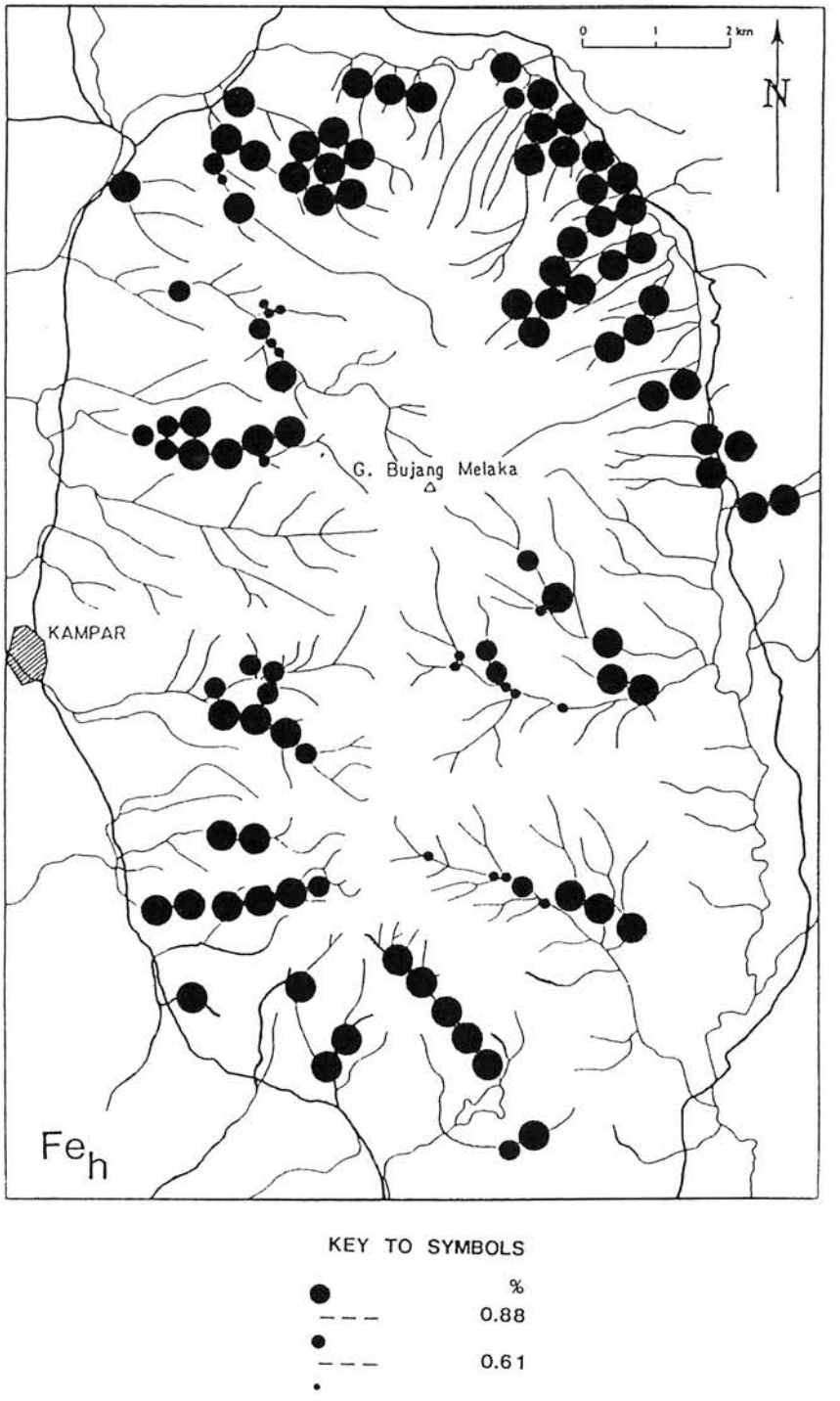

Fig. 16 Distribution of Fe in minus 80-mesh fraction, high energy environments.

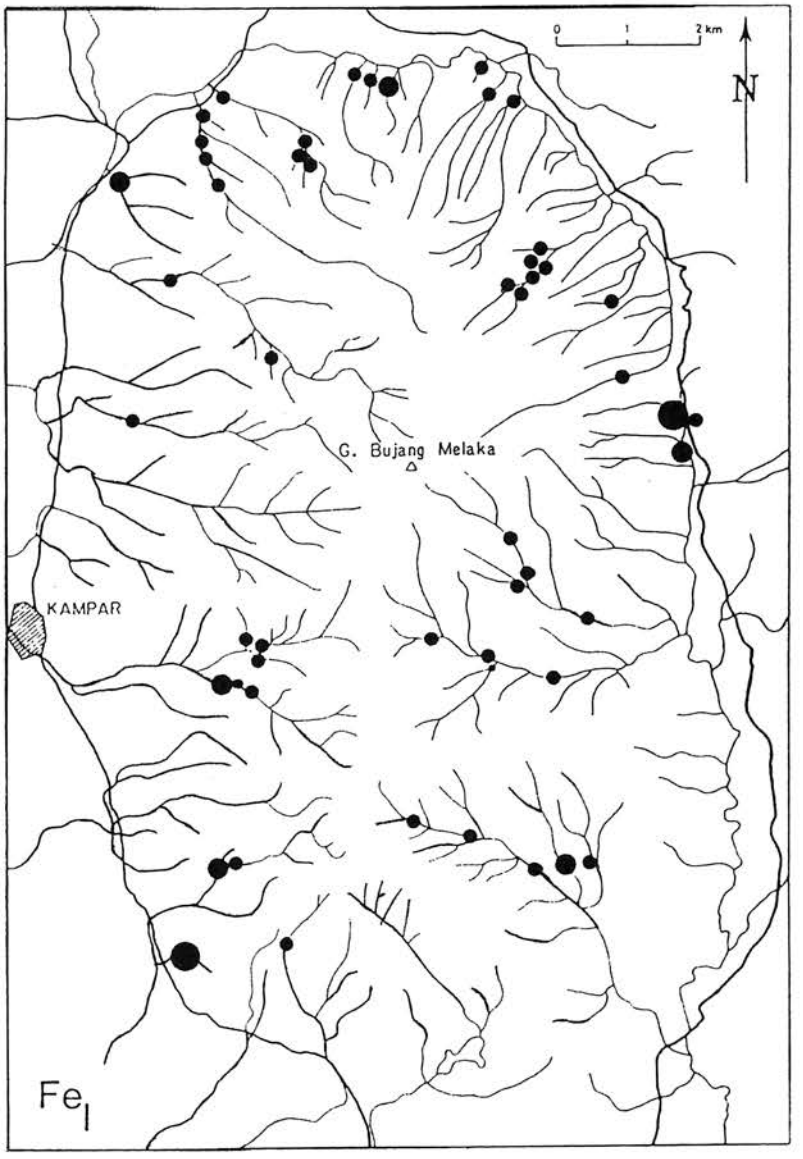

KEY TO SYMBOLS

	%
$\bar{x}+2s$	3.30
$\bar{x}+s$	1.94
$\bar{x}-s$	0.68
$\bar{x}-2s$	0.39

Fig. 17 Distribution of Fe in minus 80-mesh fraction, low energy environments.

Garrett (1983) has recommended evaluation of the reliability of regional geochemical surveys using a simple 2-level analysis of variance for F, where:

$$F = \frac{\text{among-site variance}}{\text{within-site variance}},$$

and within-site variance, based on analysis of field duplicates, estimates the combined sampling and analytical variance. The larger the value of F the more significant the regional patterns. V_m, a comparable criteria suggested by Miesch (Garrett, 1983), is equal to (F-1) for paired data and should exceed 3 for geochemical patterns to be satisfactorily recognised. Applying these criteria to results from Bujang Melaka (Table 6) provides further evidence that regional variability of Sn, unlike As (and to a lesser extent the base metals), cannot be distinguished from local (sampling and analytical) variability.

Discussion

Alluvial mine workings in the surrounding valleys, and the Sn content of stream sediments and pan concentrates clearly indicate the stanniferous character of Bujang Melaka. Identifying it as such on a regional scale exploration programme would obviously present no difficulties using either standard geochemical or panning techniques. However, problems arise in identifying targets for follow-up in so far as anomalous concentrations of Sn are ubiquitous and lack any clearly defined pattern. Furthermore, as first shown by Kaewbaidhoon (1961), concentrations of both elements are consistently enriched in coarse-grained (high energy) sediments compared to finer-grained (low energy) sediments. Magnetite also exhibits this phenomenon, which clearly results from the well-known tendency of heavy minerals to accumulate in high energy environments. Advantage of this process is taken in collecting samples for dulang panning (e.g., Chand, 1981). However, in interpreting geochemical data it causes two problems:

TABLE 6
ANALYSIS OF VARIANCE BASED ON DUPLICATE FIELD SAMPLES FOR BUJANG MELAKA S.C. MIESCH'S CRITERIA, V_M, EQUALS (F-1) AND SHOULD EXCEED 3 FOR REGIONAL SIGNIFICANT PATTERNS TO BE OBTAINED

Variable	dF	F[1]
Sn	103/104	2.63
W	85/86	3.56
As	80/81	24.52
Cu	81/82	2.91
Pb	80/81	4.79
Zn	81/82	9.56
Fe	80/81	5.58
Magnetite	45/46	2.26
Sn/magnetite	45/46	3.00

[1] Based on logged data for paired variables

(i) results of duplicate sampling at the same site can be extremely erratic—with up to a twentyfold difference being observed for Sn.

(ii) as demonstrated for Ba by Sleath and Fletcher (1982), very localized hydraulic factors, rather than the regular dilution and decay of an anomalous dispersion train with distance from its source as described by Rose *et al.* (1979), determine Sn concentration at a given point. Thus, there is no relationship between magnitude of an anomaly and proximity to its source.

Under these circumstances, distribution of Sn will only provide very limited guidelines to selecting exploration targets for further work.

The problem of local hydraulic accumulation is general for any element transported as a resistate heavy mineral. However, at Ulu Petai, As is present as arsenopyrite, which is unstable and should break down in the weathering environment to give soluble products capable of being absorbed by finer fractions of the sediment. Arsenic should not, therefore, be very susceptible to hydraulic accumulation. This appears to be the case in so far as (i) differences in As concentrations between low and high energy environments are not significant (Table 4), and (ii) in the Sungei Palai and Sungei Kinchap, As anomalies do appear to be diluted downstream. Thus, it seems likely that anomalous concentrations of As in sediments could indicate relative proximity to Sn mineralisation of the type found at Ulu Petai.

Regional data therefore confirms the influence of hydraulic effects on the dispersion of Sn and also suggests that As might be used as a pathfinder. On the basis of these results, detailed studies were undertaken on the Sungei Petai to (1) find methods of minimising the influence of hydraulic conditions on Sn, and (2) investigate As and other potential pathfinders. These studies are reported in the next section.

BEHAVIOUR OF TIN AND ASSOCIATED ELEMENTS IN THE SUNGEI PETAI

Detailed orientation studies of the behaviour of Sn and associated elements were undertaken in the Sungei Petai downstream of the abandoned Ulu Petai mine workings (Figure 5). Initial studies involved routine collection and analysis of minus 80-mesh material followed by investigation of the distribution of Sn in different size fractions of bulk sediments from high and low energy environments.

Results

Composition of minus 80-mesh sediments

Sediment geochemical data are summarized in Figures 18-23 and for magnetite in Figure 24. Several features are consistent with the regional data, and it is particularly interesting to note that even in proximity to the Ulu Petai mine concentrations of Sn do not exceed the upper limit of their regional background values for Bujang Melaka (Table 4). In contrast, anomalous concentrations of Cu, Pb and Zn exceed regional threshold values as far as 1 km downstream from the Ulu Petai lodes. Beyond this point, dilution by two major tributaries entering the Sungei Petai at Station 19 eliminates the anomalies. Enhanced As values, exceeding 66 ppm ($\bar{x}$ + s, low energy sites), also disappear below this point.

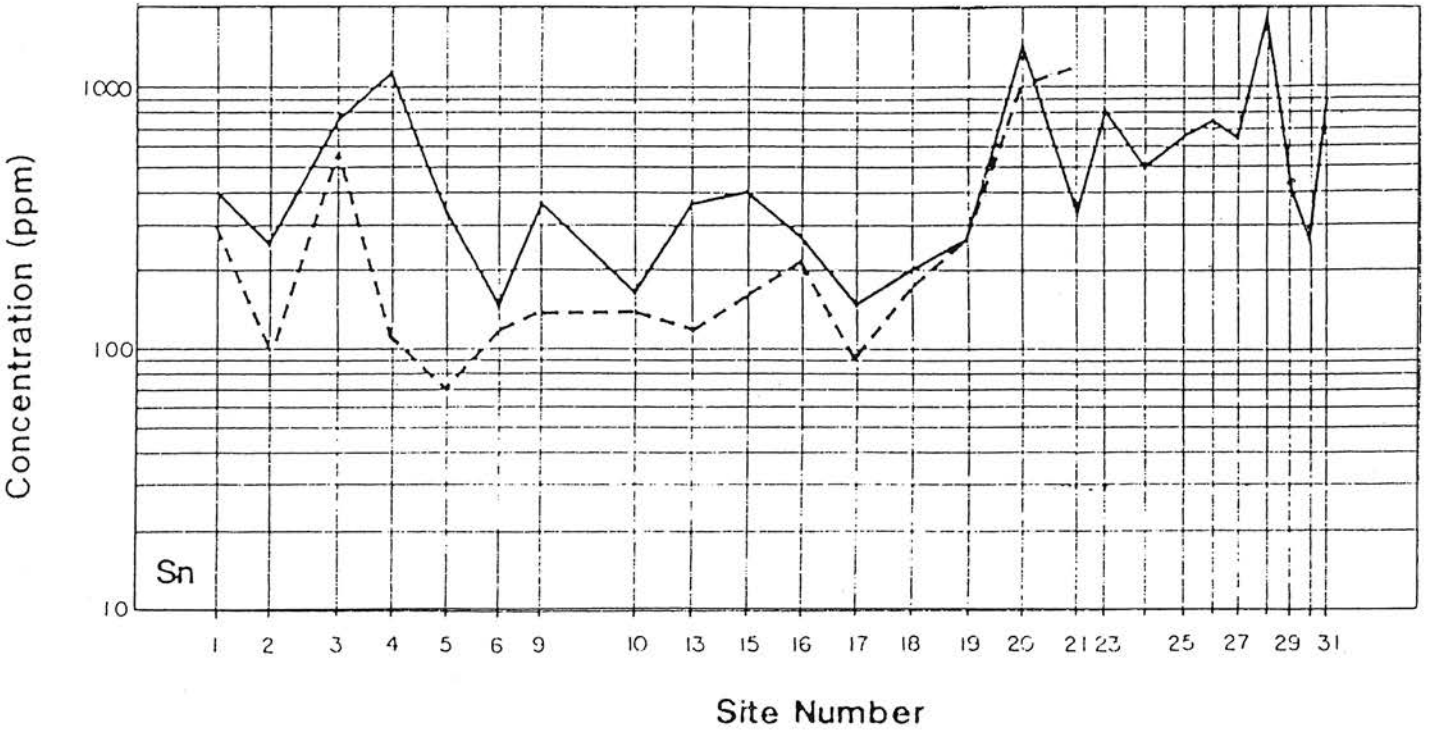

Fig. 18 Distribution of Sn in minus 80-mesh sediments from high (—) and low (---) energy environments, Sungei Petai.

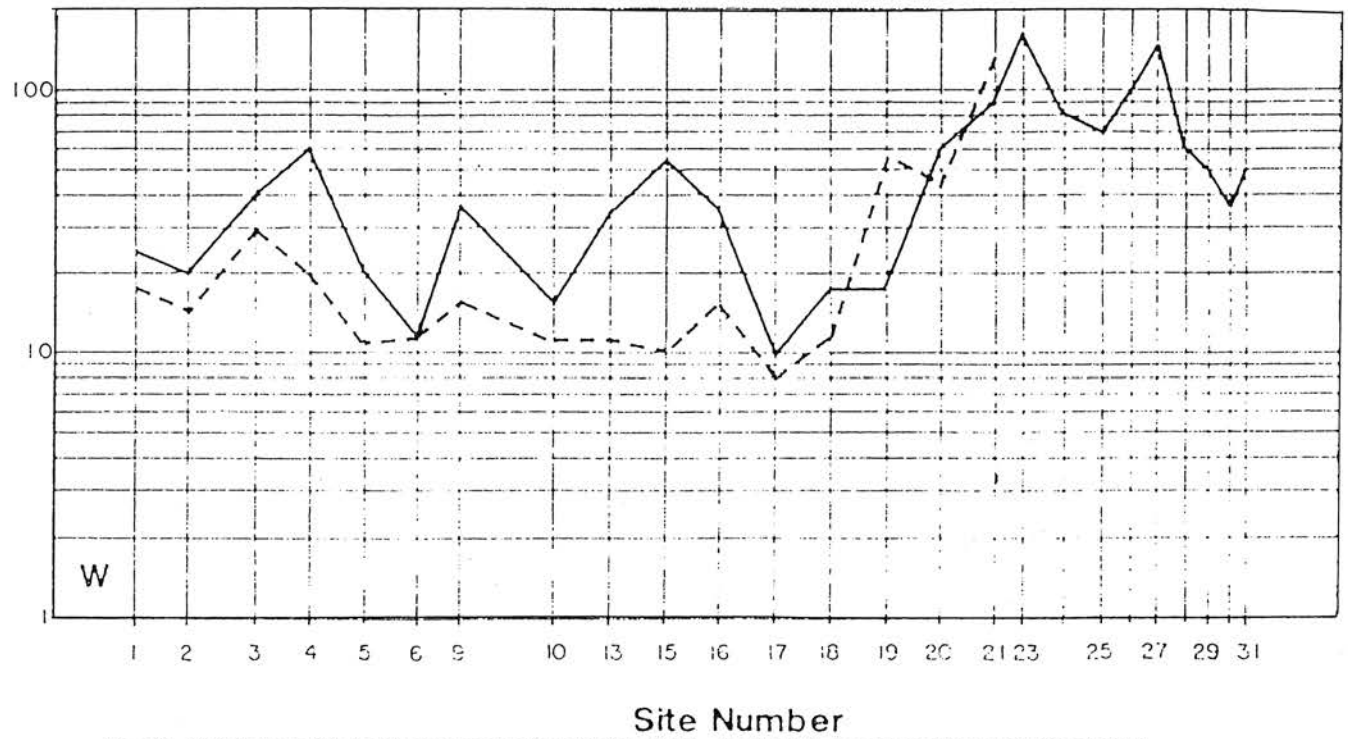

Fig. 19 Distribution of W in minus 80-mesh sediments from high (—) and low (---) energy environments, Sungei Petai.

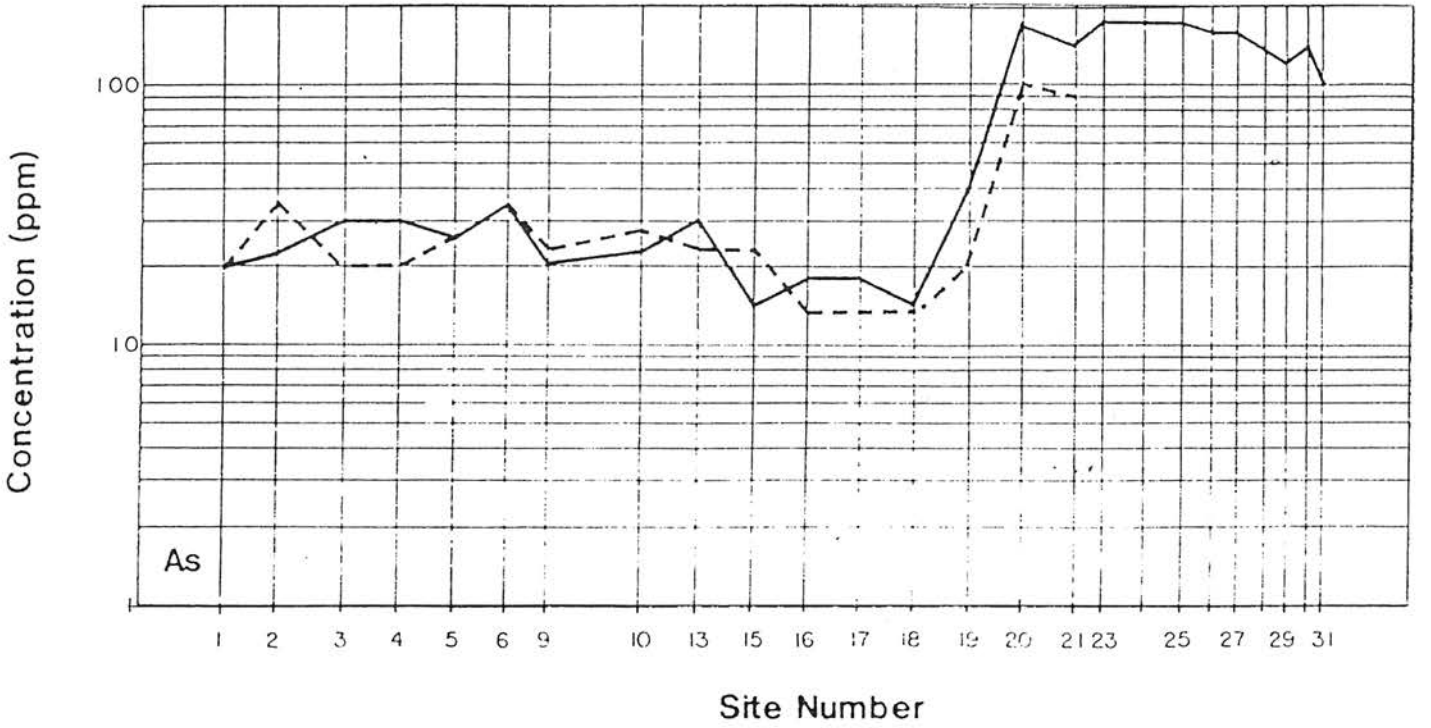

Fig. 20 Distribution of As in minus 80-mesh sediments from high (—) and low (---) energy environments, Sungei Petai.

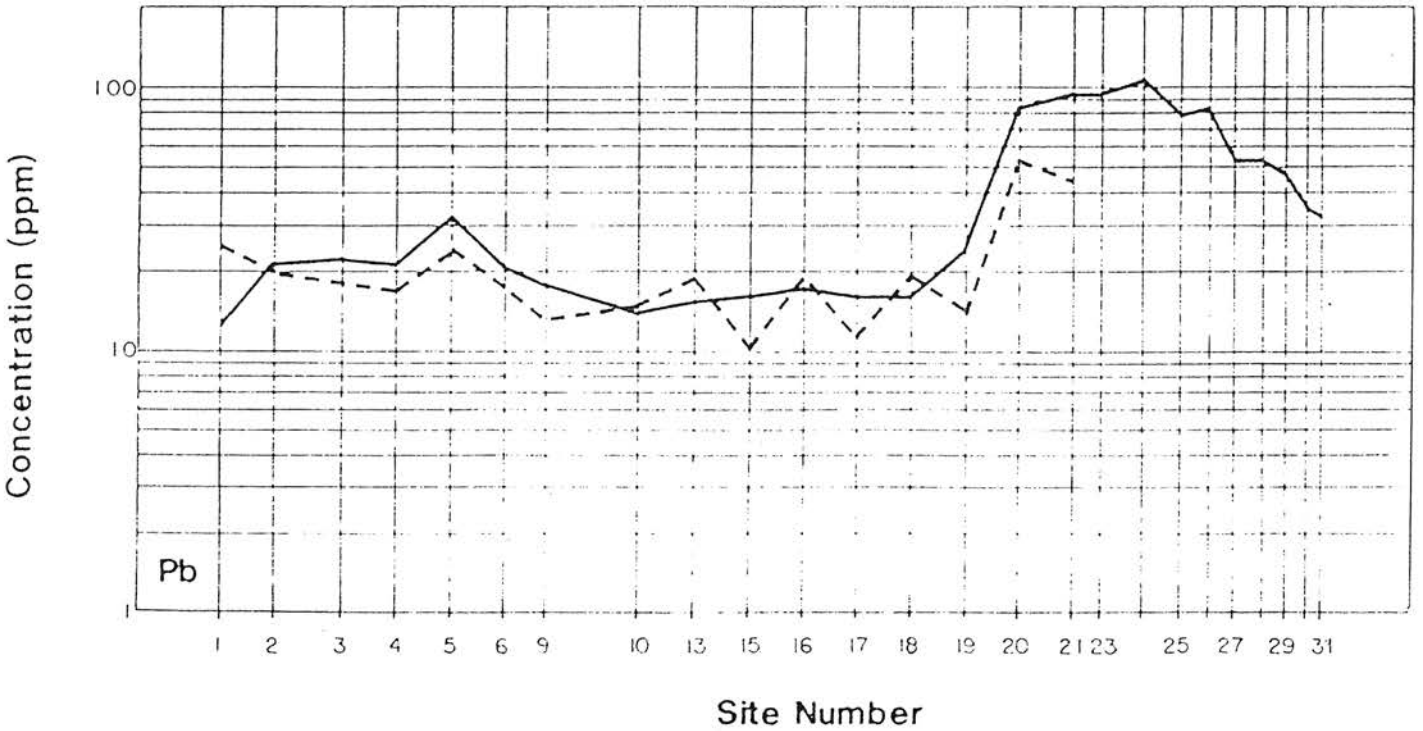

Fig. 21 Distribution of Pb in minus 80-mesh sediments from high (—) and low (---) energy environments, Sungei Petai.

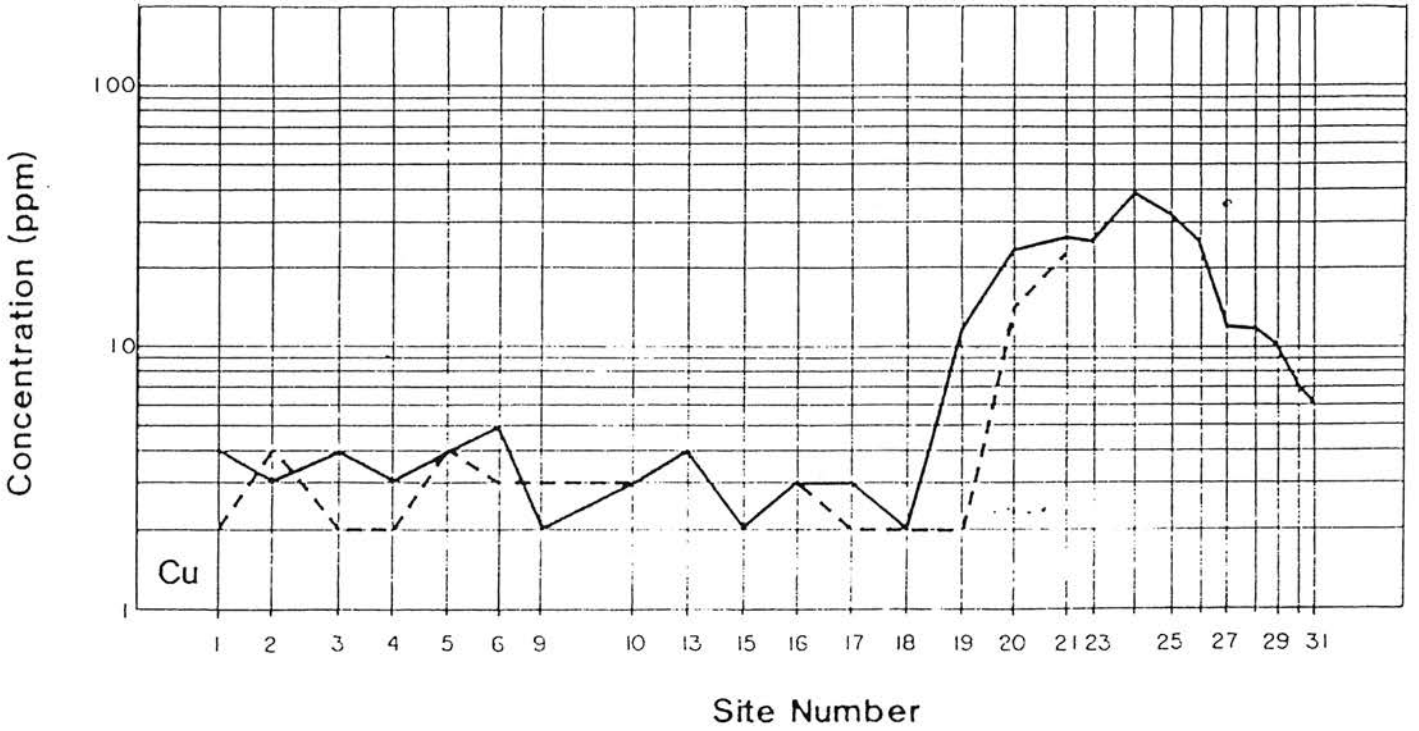

Fig. 22 Distribution of Cu in minus 80-mesh sediments from high (—) and low (---) energy environments, Sungei Petai.

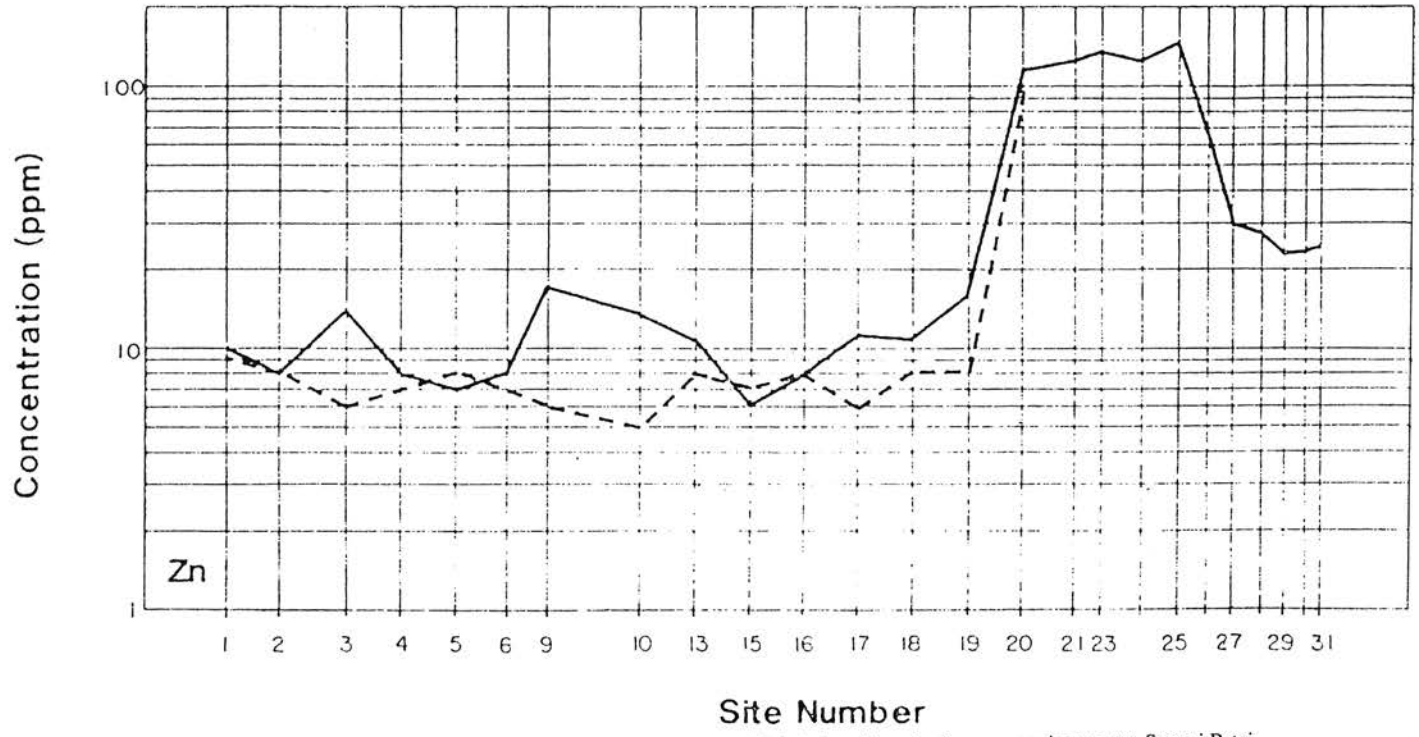

Fig. 23 Distribution of Zn in minus 80-mesh sediments from high (—) and low (---) energy environments, Sungei Petai.

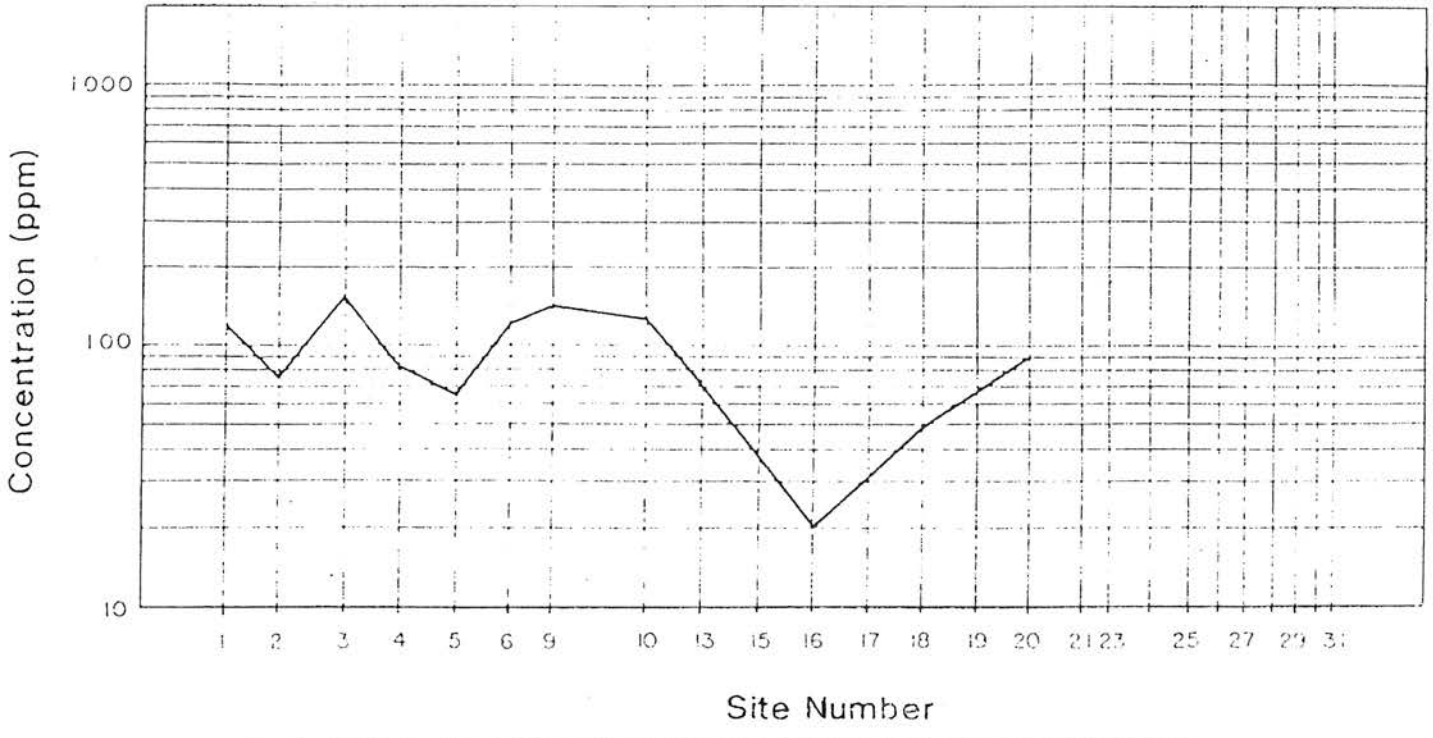

Fig. 24 Distribution of magnetite in minus 80-mesh sediments from low energy environments, Sungei Petai.

Unlike the base metals and As, high concentrations of Sn are found both near Ulu Petai and again downstream at Stations 3 and 4. Results vary very erratically between stations but, as in the regional data, concentrations are almost invariably greater at high energy sites than at corresponding low energy sites. Data for W show the same features, and there is a general and remarkably close correspondence between behaviour of the two elements. This leads to a correlation coefficient of 0.77 between Sn and W at low energy sites. Downstream of Station 10 there is also a close relationship between Sn and magnetite concentrations (Figures 18 and 24).

Size fraction studies

In both the regional survey and comparable minus 80-mesh data for the Sungei Petai, similarities in behaviour of Sn, W and magnetite indicate the importance of the local hydraulic environment in concentrating heavy minerals. Detailed studies were therefore made of the behaviour of Sn in eight different size fractions during transport down the Sungei Petai. Magnetite was also determined in one (minus 65+100 mesh) of these fractions.

Results (Figures 25 to 32) show major differences between Sn content of the same size fraction at low and high energy sites and between size fractions. Thus:

1. For all size fractions, maximum concentratins of Sn (1000 ppm) are found in proximity to the mineralization at Ulu Petai and downstream as far as Station 20. Along this part of the Sungei Petai, low energy environments are absent and duplicate pairs of high energy environments have similar contents.

2. Downstream from station 20, Sn concentrations at high energy sites are often considerably greater than at corresponding low energy sites. This difference is greatest in the coarse size fractions and gradually decreases with decreasing grain size until it is no longer apparent in the finest (minus 270 mesh) fraction (Table 7).

3. Particularly in the coarser size fractions, Sn content of high energy sites is extremely erratic and concentrations at Stations 3, 4 and 6 are comparable to those at Ulu Petai. In contrast, Sn values at low energy sites show a more uniform decay downstream of Ulu Petai and relatively little variation below Station 15.

4. Reduction in the difference between Sn content of high and low energy sites, as grain size decreases, results from a concomitant increase in Sn content of the latter.

These variations in distribution of Sn among the size fractions and between high and low energy sites are most apparent between Stations 1 and 15. A statistical summary (Table 7) for this section of the river clearly show (i) the gradual increase in Sn content with decreasing grain size (to a maximum in the minus 200+270-mesh fraction) for low energy environments, and (ii) the higher coefficients of variation associated with all but the two finest size fractions in the high energy environment. A paired t-test between the environments indicates that, except in the minus 270-mesh fraction, average Sn contents of high energy sites are significantly greater than those of low energy sites.

TABLE 7
COMPARISON OF TIN CONTENT (PPM) OF VARIOUS SIZE FRACTIONS OF SEDIMENTS FROM HIGH AND LOW ENERGY ENVIRONMENTS IN THE SUNGEI PETAI BETWEEN STATIONS 1 AND 15

Size fraction	Environment		t[1]
	High energy	Low energy	
– 270	252[2] 24[3]	260 38	-0.24
– 200 + 270	513 38	320 54	2.22
– 150 + 200	695 63	245 41	3.02
– 100 + 150	543 60	144 35	3.69
– 65 + 100	323 95	65 55	2.85
– 48 + 65	308 78	41 55	3.48
– 35 + 48	229 169	30 27	1.62
– 28 + 35	212 171	27 32	1.63

[1] t with 9 df $t_{.99} = 2.821$ $t_{.95} = 1.833$ $t_{.90} = 1.383$
[2] Arithmetic mean (ppm)
[3] Coefficient of variations (%)

Size distribution of Sn can also be considered in relation to the bulk size distribution of each sample (Figures 33 to 35). When presented in this way it is apparent that Sn shows a strong preferential association with the finer size fractions, to the extent that in many samples, the first (finest) ten percent of the bulk sediment contains more than ninety percent of the relative Sn content. Exceptions to this are samples from Stations 27 to 30, at Ulu Petai, and downstream and at Stations 2 and 6, all of which have less than seventy percent of their relative tin content in the first ten percent of the bulk sediment. Downstream of Station 27 the change in relative proportions of Sn corresponds to a shift of its modal value from minus 65+100 mesh to finer size fractions.

Magnetite minus 65+100-mesh fraction

Magnetite concentrations in the minus 65+100-mesh fraction are similar in duplicate pairs from high energy sites in the headwaters of the stream. Further downstream, magnetite—like Sn—is preferentially concentrated at high energy sites (Figure 36). Thus, between Stations 1 and 15, mean values for high and low environments are 215 ppm and 46 ppm, respectively. This difference is significant at the 1% level. Results also resemble those for Sn in that magnetite content of high energy sites is much more erratic than at low energy sites. Major

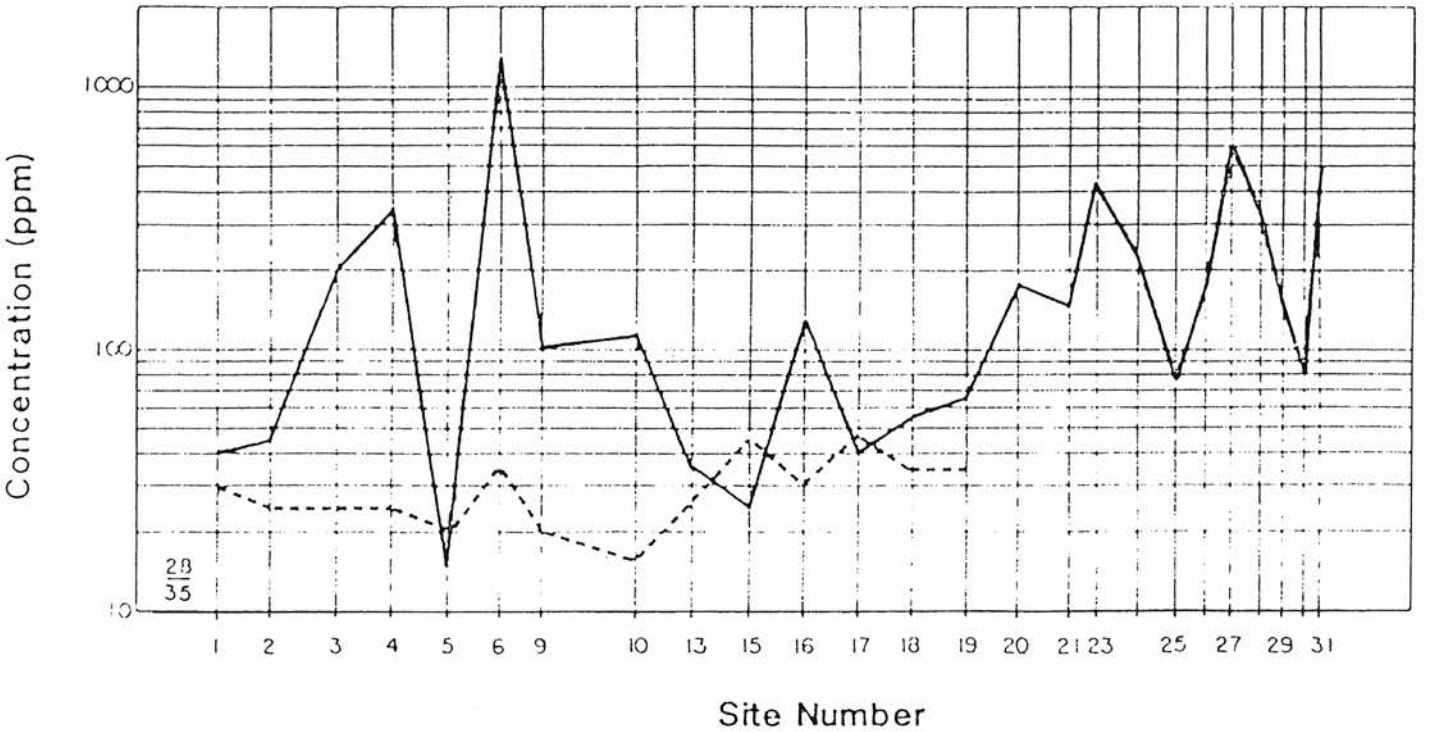

Fig. 25 Distribution of Sn in minus 28 + 35 -mesh fraction of sediments from high (—) and low (---) energy environments, Sungei Petai.

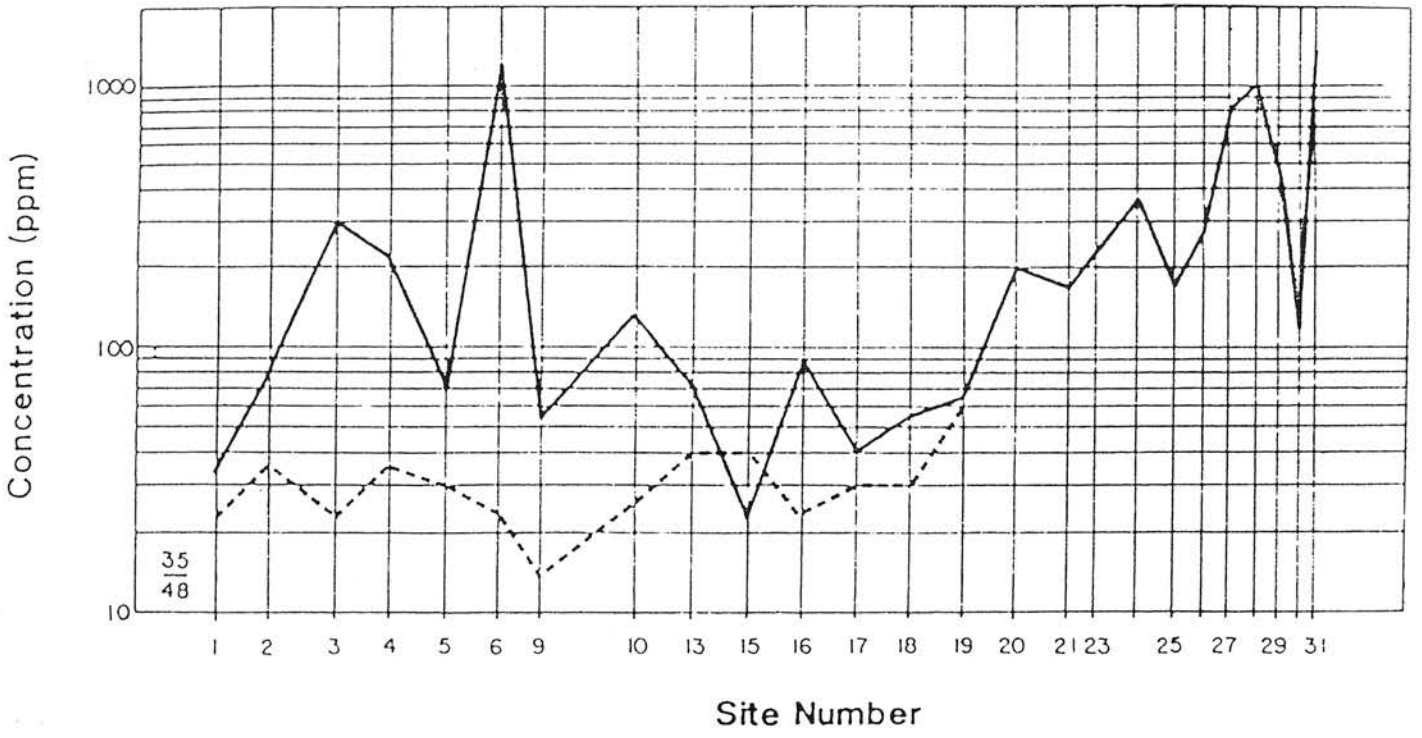

Fig. 26 Distribution of Sn in minus 35 + 48 -mesh fraction of sediments from high (—) and low (---) energy environments, Sungei Petai.

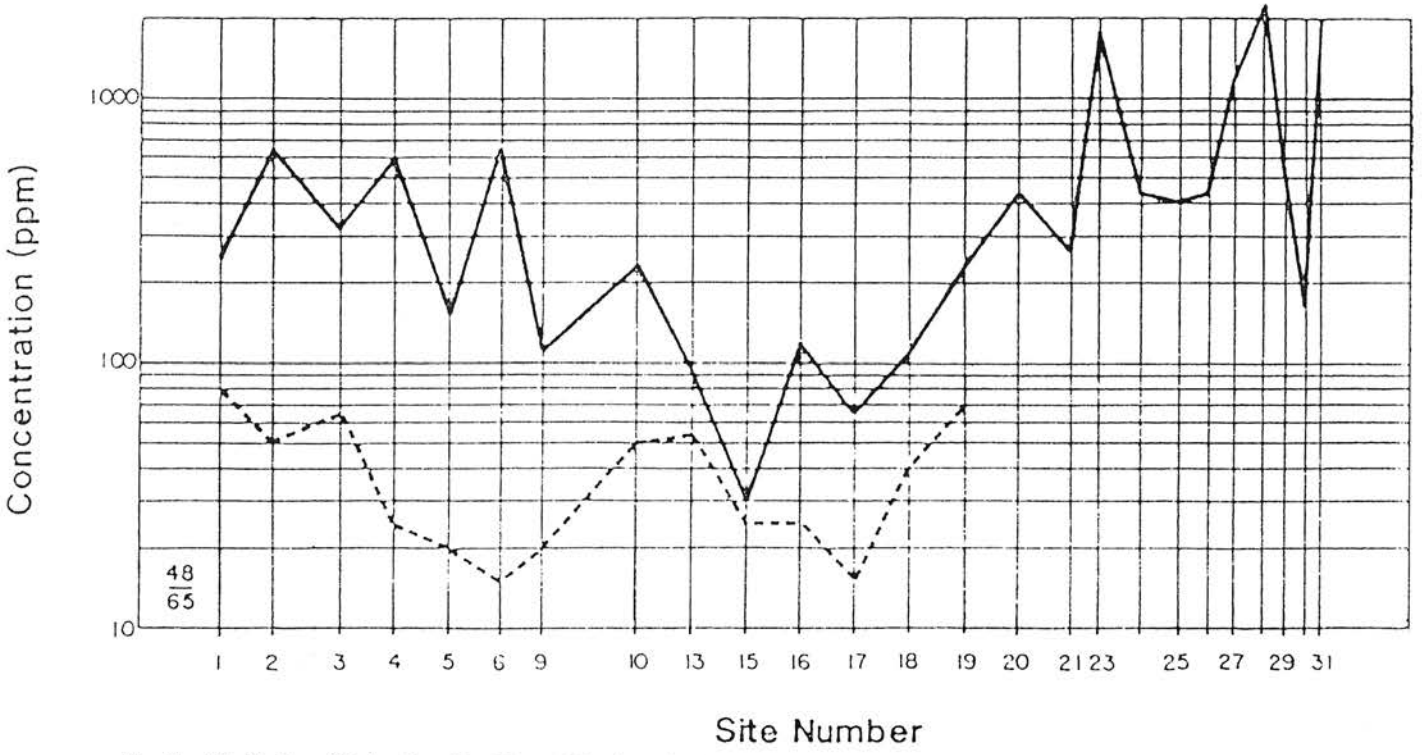

Fig. 27 Distribution of Sn in minus 48 + 65 -mesh fraction of sediments from high (—) and low (---) energy environments, Sungei Petai.

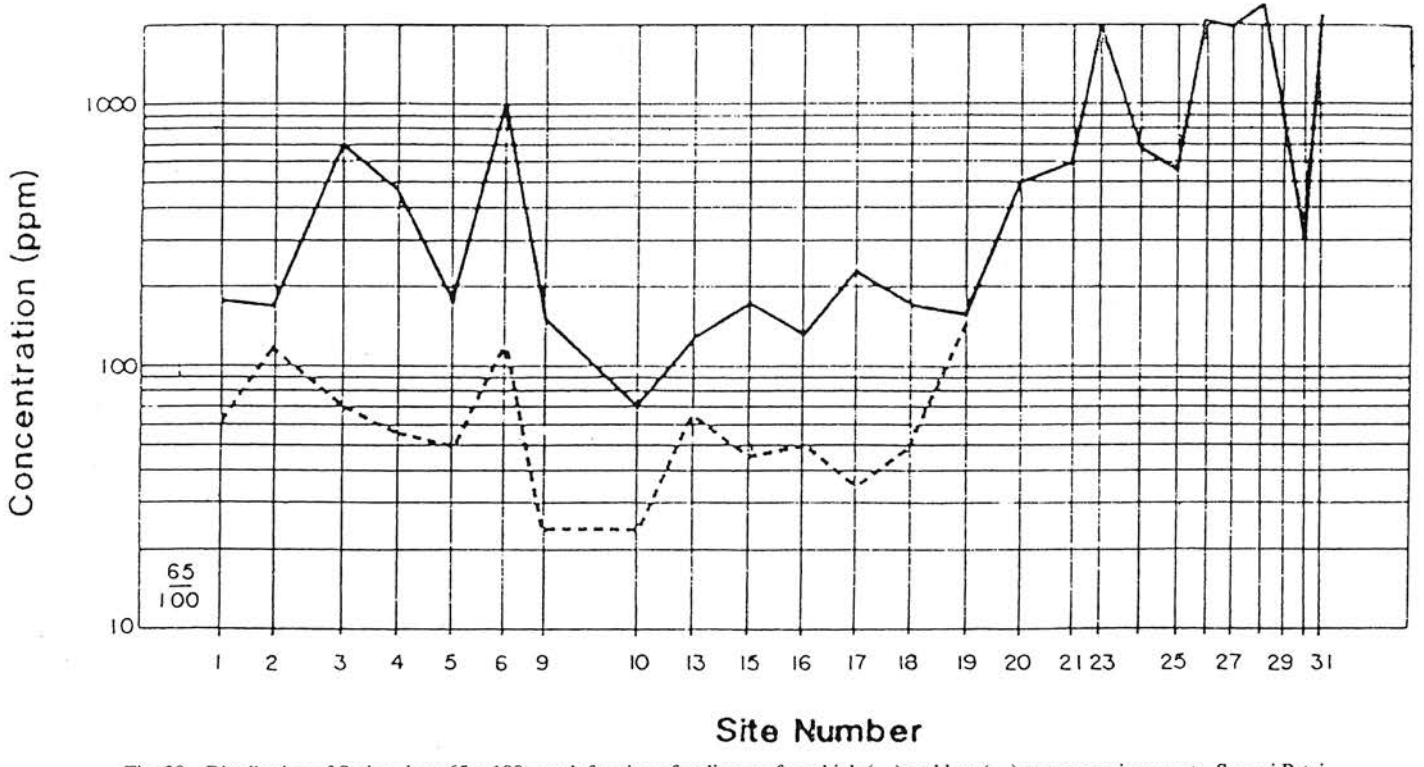

Fig. 28 Distribution of Sn in minus 65 + 100 -mesh fraction of sediments from high (—) and low (---) energy environments, Sungei Petai.

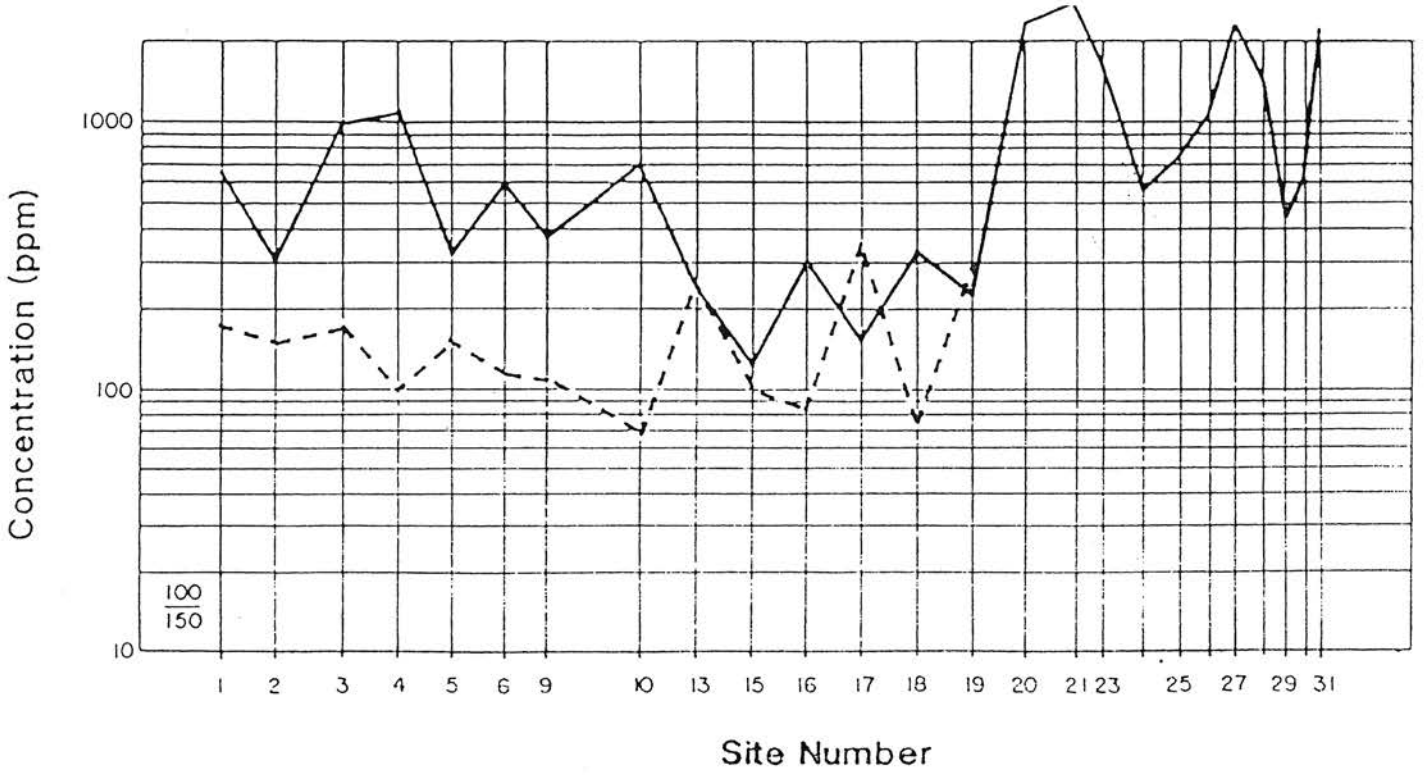

Fig. 29 Distribution of Sn in minus 100 + 50 -mesh fraction of sediments from high (—) and low (---) energy environments, Sungei Petai.

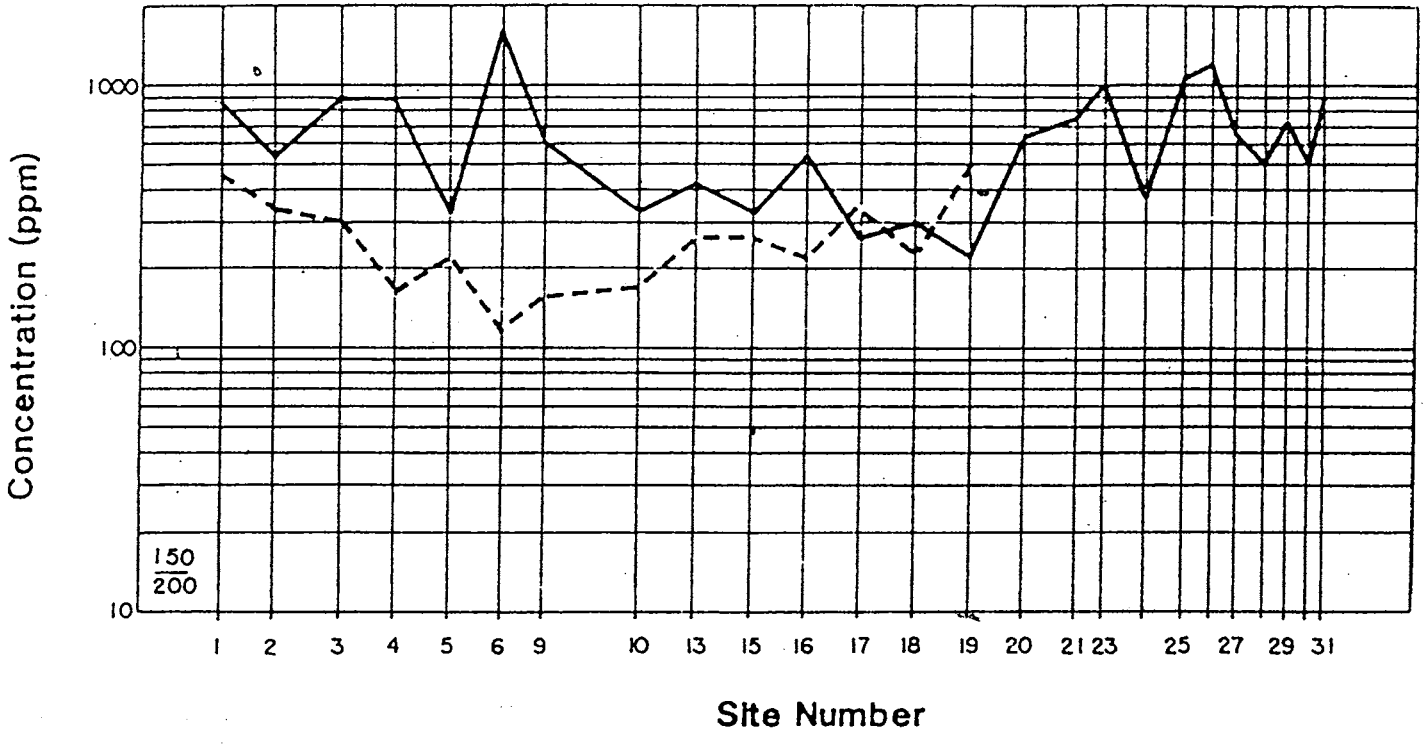

Fig. 30 Distribution of Sn in minus 150 + 200 -mesh fraction of sediments from high (—) and low (---) energy environments, Sungei Petai.

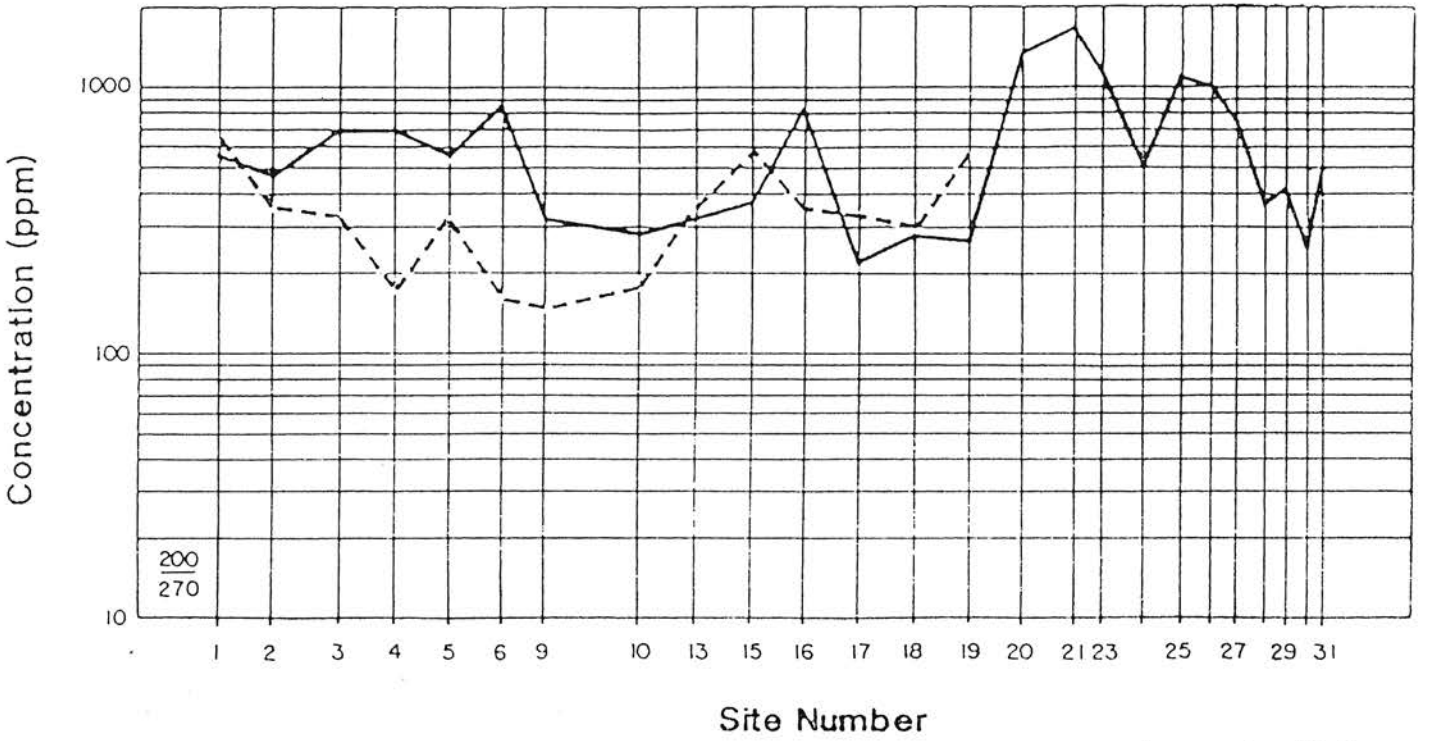

Fig. 31 Distribution of Sn in minus 200 + 270 -mesh fraction of sediments from high (—) and low (---) energy environments, Sungei Petai.

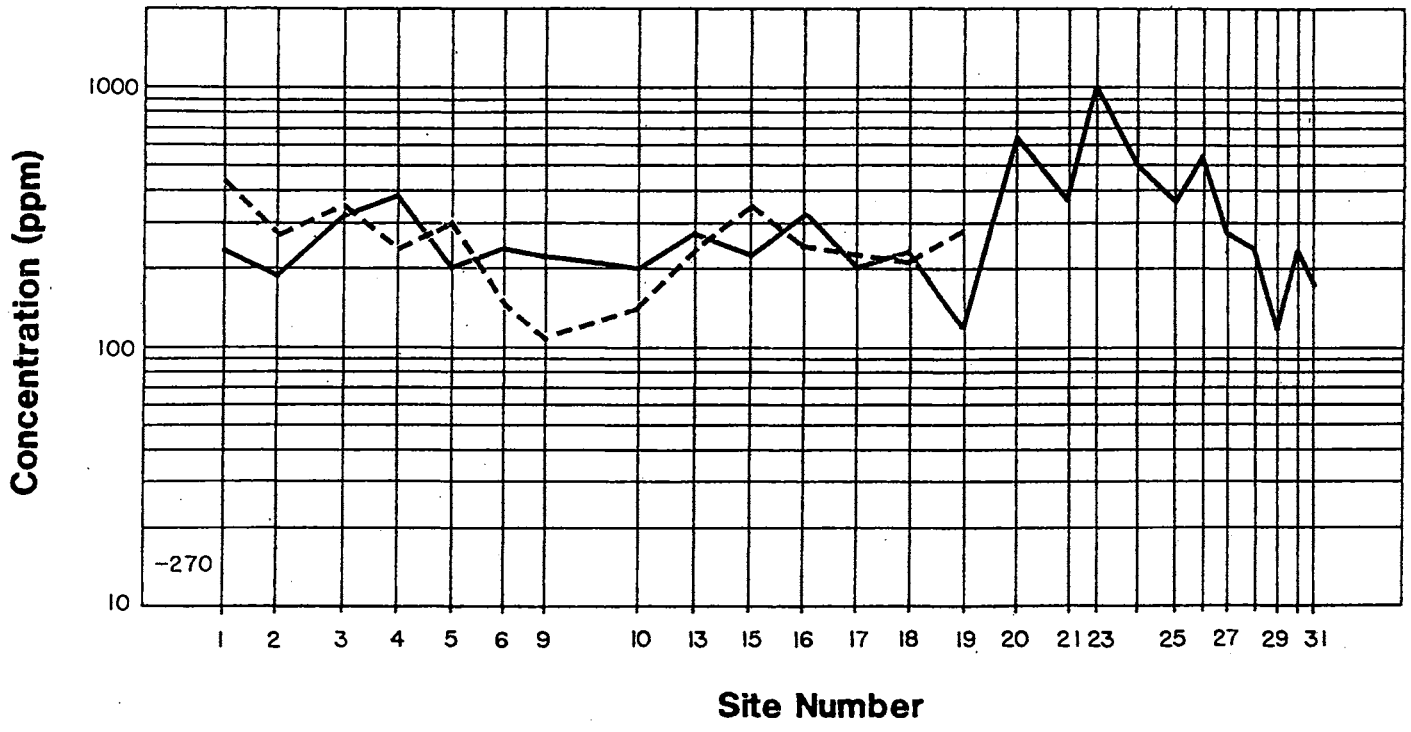

Fig. 32 Distribution of Sn in minus 270 -mesh fraction of sediments from high (—) and low (---) energy environments, Sungei Petai.

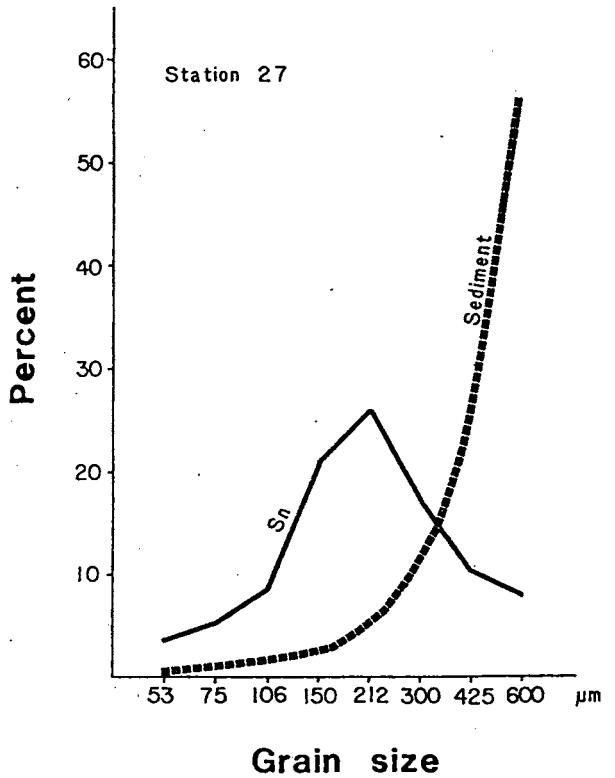

Fig. 33 Relationship between size distribution Sn and bulk sediment, high energy environment Station 27.

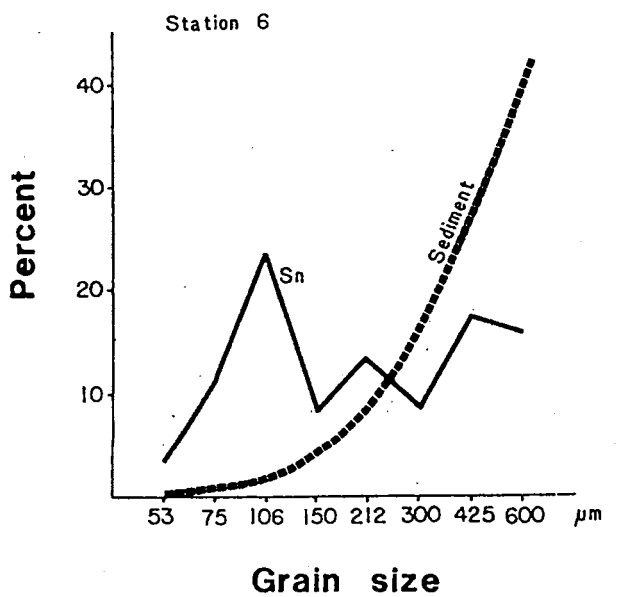

Fig. 34 Relationship between size distribution Sn and bulk sediment, high energy environment Station 6.

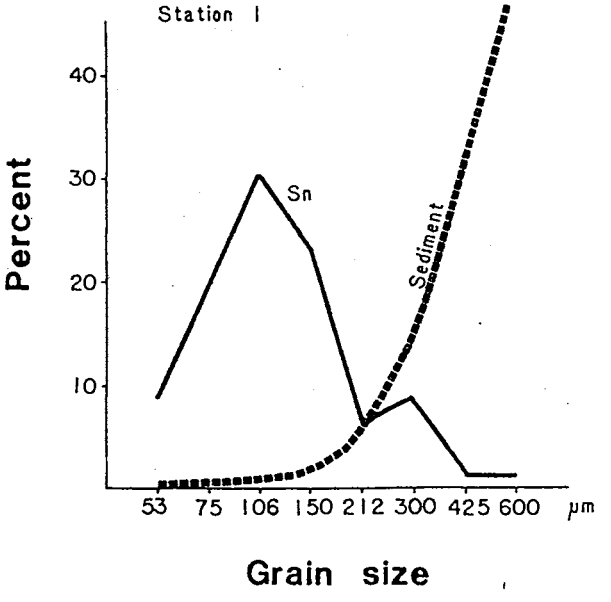

Fig. 35 Relationship between size distribution Sn and bulk sediment, high energy environment Station 1.

accumulations of magnetite in high energy sediments at Stations 4 and 6 are particularly striking.

Heavy mineral concentrates

Principal heavy minerals in *dulang* concentrates of the Sungei Petai are tourmaline and ilmenite, the latter predominating in concentrates from the lower part of the river but decreasing to minor quantities in the headwaters (Figure 37). Minor quantities (less than ten percent) of zircon, rutile and monazite are also present with traces of xenotime, leucoxene and topaz. Based on visual estimates, cassiterite content ranges from trace to 0.288 katis per cubic yard (kpcy)[1], with values in excess of 0.1 kpcy at Stations 15, 16 and 23 (Table 8). Corresponding chemical assays have tin contents from 0.65 to 32.5% SnO_2.

Discussion

As noted in the discussion of regional results, the principal geochemical exploration problem on Bujang Melaka is to identify priority targets within a large regional anomaly characterized by very erratic Sn data. Detailed studies on the Sungei Petai corroborate the regional study and confirm that base metal (Cu, Pb and Zn) anomalies and enhanced As concentrations are associated with tin mineralization at Ulu Petai. The anomalous dispersion

[1] $1 kg/m^3 = 1.264$ kpcy

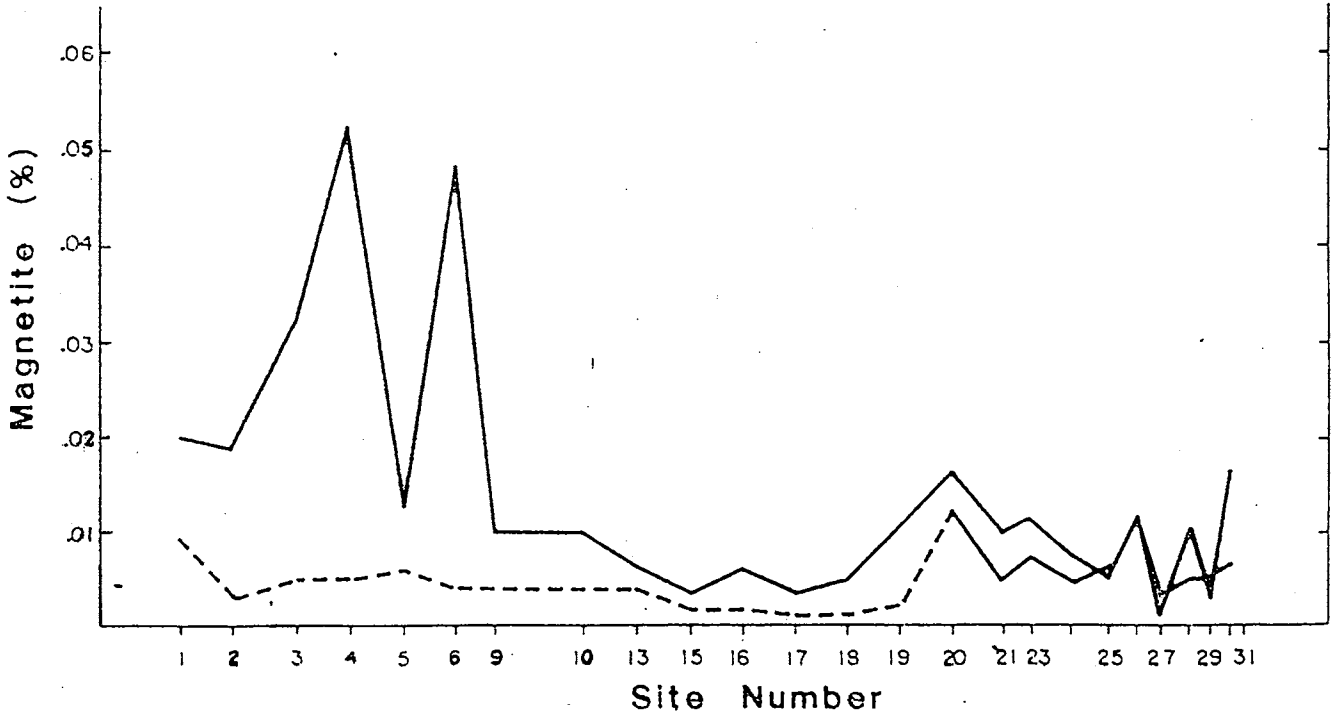

Fig. 36 Distribution of magnetite in minus 65-plus 100 -mesh fraction of sediments from high (—) and low (---) energy environments, Sungei Petai.

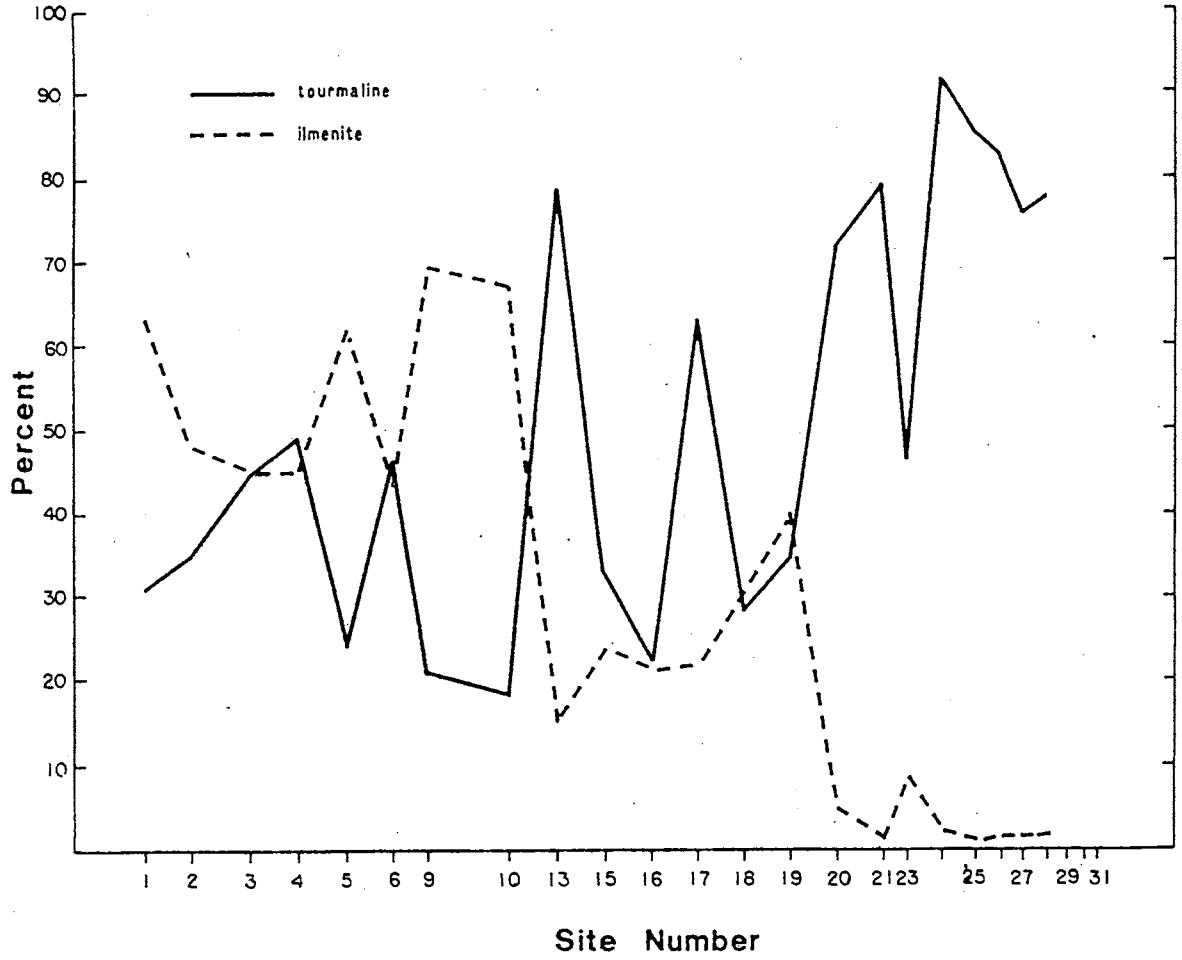

Fig. 37 Distribution of ilmenite and tourmaline in *dulang* concentrates, Sungei Petai.

TABLE 8
TIN CONTENT OF *DULANG* CONCENTRATES, SUNGEI PETAI

Site #	Weight[1] (g)	SnO_2% [2]	Sn kpcy[3]
1	4.92	1.22	Tr
2	4.08/4.26	1.88/4.04	Tr/0.063
3	3.78	0.90	Tr
4	1.26	2.43	Tr
5	1.14	0.86	Tr
6	1.66	2.27	0.003
9	2.56	1.78	0.004
10	2.69	1.47	0.007
13	0.76	0.65	0.003
15	1.94	20.07	0.138
16	2.18	32.51	0.288
17	0.55	2.36	0.001
18	1.55	12.83	0.08
19	1.56	7.21	0.006
20	2.15	7.80	0.05
21	1.39	2.34	0.007
23	2.39	20.70	0.196
24	1.80	0.94	0.005
25	1.71	3.76	0.005
26	1.65	3.99	0.004
27	1.67	8.10	0.05
28	1.47	6.93	0.03

[1] g of concentrate per standard *dulang* = 0.00616 yd^3
[2] Chemical assay
[3] Visual estimates from concentrates after cleaning with bromoform: kpcy = 0.027 x %SnO_2 x g concentrate/number of *dulangs*

trains extend approximately one kilometre downstream from their source to Station 19, where they are eliminated at the confluence of the Sungei Petai, with two major tributaries. Each of these elements is known to occur in the primary mineralization at Ulu Petai as sulphide minerals (Ingham and Bradford, 1960; Riley, 1968). Their value as pathfinders therefore presumably reflects their release, as the sulphides are decomposed during weathering, and subsequent dispersion in drainage sediments in phases (probably adsorbed on finer fractions of the sediment) that are not influenced by variations in local hydraulic conditions.

Examination of heavy mineral concentrates suggests that an abundance of tourmaline and a relatively low content of ilmenite might also be useful guides to proximity of the primary source (Figure 37). However, for other types of tin mineralization, both on Bujang Melaka and elsewhere, suitable pathfinder elements or mineralogical guides might be unavailable. The remainder of this discussion is therefore aimed at understanding factors influencing dispersion of Sn, as cassiterite, in drainage sediments and developing criteria whereby the influence of varying hydraulic conditions on tin content of sediments can be identified and corrected for.

Concentration of Sn (and W) in the Sungei Petai are above average but not anomalous for Bujang Melaka. Furthermore, they are strongly influenced by local hydraulic conditions with the highest concentrations, as reported by Kaewbaidhoon (1961), in high energy environments. Presumably the supply of cassiterite to neighbouring high and low energy environments is essentially the same. Differences between such sites must, therefore, reflect the ability of stream flow to selectively transport and winnow away light minerals leaving the remaining sediment relatively enriched in Sn.

Comparisons of regional background results (Table 9) and data for the coarsest size fraction analysed (minus 28+35 mesh) suggest that Sn is not enriched in this fraction in low energy environments of the Sungei Petai. In contrast, Sn content of high energy minus 28+35-mesh sediments can be enhanced more than twentyfold. Thereafter, in all finer size fractions except minus 270 mesh, average Sn content progressively increases with decreasing grain size for both high and low energy environments. This no doubt partly reflects the slight increases in background Sn concentrations reported for the finer size fractions in Table 9. However, a more important factor is the increasing ability of the stream to selectively transport light minerals as grain size diminishes. In so far as this ability varies considerably with local hydraulic conditions, resulting accumulations of cassiterite increase sampling variability at each site and disrupt the regular decay of anomalous Sn concentrations downstream from their source. For example, the enhanced Sn values at Stations 3, 4 and 6 Figures 25 to 30) almost certainly reflect hydraulic accumulation of cassiterite in that:

(1) they are largely confined to high energy environments (thereby increasing sampling variance);
(2) base metal and As anomalies are absent; and
(3) associated bank soils do not contain anomalous concentrations of Sn (Table 10).

Sleath and Fletcher (1982) and Gladwell (1981) have shown that hydraulic effects for heavy minerals can be corrected by utilizing their relationship to other, hydraulically equivalent, minerals. In the present case, the obvious similarity between behaviour of Sn and

TABLE 9
SN CONTENT (PPM) OF VARIOUS SIZE FRACTIONS OF SEDIMENTS FROM BACKGROUND STREAMS DRAINING THE MAIN RANGE GRANITE EAST OF BUJANG MELAKA (N=4)

Size fraction mesh	High energy	Low energy
270	61[1]	54
	50-80	45-60
200+270	59	78
	50-65	60-120
150+200	73	86
	50-110	45-170
100+150	78	74
	20-150	40-120
65+100	58	58
	25-110	50-80
48+65	43	40
	25-60	30-50
35+48	34	35
	25-45	30-40
28+35	28	30
	20-40	15-50
20+28	33	
	25-45	–

[1] Arithmetic mean and range

magnetite (Table 4) suggests that the Sn/magnetite ratio might be effective. This is confirmed by a plot of Sn/magnetite for the minus 65+100-mesh fraction along the Sungei Petai (Figure 38) in which anomalies at Stations 3, 4 and 6 are eliminated and contrast for anomalous sediments near the source at Ulu Petai is enhanced. At the same time, differences between high and low energy environments at the same station are reduced. These combined effects can be quantitatively evaluated using the variance ratio (F), which increases from 4.7 for the original Sn data to 7.9 for the Sn/magnetite ratio. Reduction of within-site variability for Sn/magnetite compared to Sn is also apparent in the regional data (Table 4).

The foregoing suggests that Sn/magnetite ratios could be a useful interpretive aid: Sn anomalies near their primary source would have relatively high ratios, whereas for enhance values resulting from hydraulic accumulation, the ratio would be lower. At the same time

differences between high and low energy environments at the same station are minimized, thereby reducing the contribution of sampling errors to data variability. However, use of the ratio assumes a ubiquitous distribution and steady supply of magnetite to drainage sediments of the area surveyed. Regional variations in supply of maghetite and especially associatiion of magnetite with tin mineralization, as in many skarn deposits, could produce misleading results.

In view of the potential limitations in use of the Sn/magnetite ratio, it would be useful if the concept of hydraulic equivalence could be extended from cassiterite-magnetite to a relationship between cassiterite and the light minerals, principally quartz and feldspar, that constitute the bulk of the sediment.

Gladwell (1981), studying behaviour of cassiterite in streams in southwest England, found systematic changes in the relative size distributions of cassiterite and light minerals with distance from the primary source (Figure 39). These changes enabled him to develop criteria for distinguishing near source and environmental accumulations of Sn. However, the procedure is relatively cumbersome, requiring complete size fraction analyses of all sediment samples. Furthermore, preliminary attempts to apply it in the Sungei Petai (Figures 40-42) suggests that there are no major changes in relative size distributions of cassiterite and lights with distance downstream, all the curves being similar to Gladwell's background curve (Figure 39C). Hence, his procedures do not appear to be applicable in this case.

This study has therefore taken a different approach to the problem of hydraulic equivalence of cassiterite to grains of light minerals, Assume that grains of cassiterite of one size are hydraulically equivalent to quartz grains of a different diameter. By definition, these grains will behave in the same way during their transport along a stream. Consequently, the ratio between cassiterite and the hydraulically equivalent grains of quartz can only change (assuming no comminution and no chemical reactions) as a result of either additional inputs of cassiterite or dilution resulting from addition of more quartz. We will refer to this ratio as the hydraulic equivalent concentrations (HEC) of Sn and calculate its value as follows:

$$ {}_{x}HEC_{y} = \frac{Sn_{x}.W_{x}}{W_{y}} $$

where Sn_x is the concentration (ppm) of Sn in size fraction x (weight W_x) and W_y is the weight of the (coarser) fraction of quartz hydraulically equivalent to the cassiterite in fraction x.

The practical problem is to establish what (if any) grain sizes of cassiterite and light minerals are hydraulically equivalent. For diameters less than 0.2 mm, Stokes law predicts that a sphere with the density of cassiterite would settle through a column of water at the same speed as a sphere of quartz having approximately twice its diameter (Tourtelot, 1968). However, under real flow conditions along a stream bed, the lhydraulic equivalence of entrainment, rather than settling, is required. This is a very much more complex concept that as yet no theoretical model is capable of predicting [see, for example, Grigg and Rathbun (1969); McQuivey and Keefer (1969); Brady and Jobson (1973); Hand (1976); Lowright *et al.* (1972); and Slingerland (1977)].

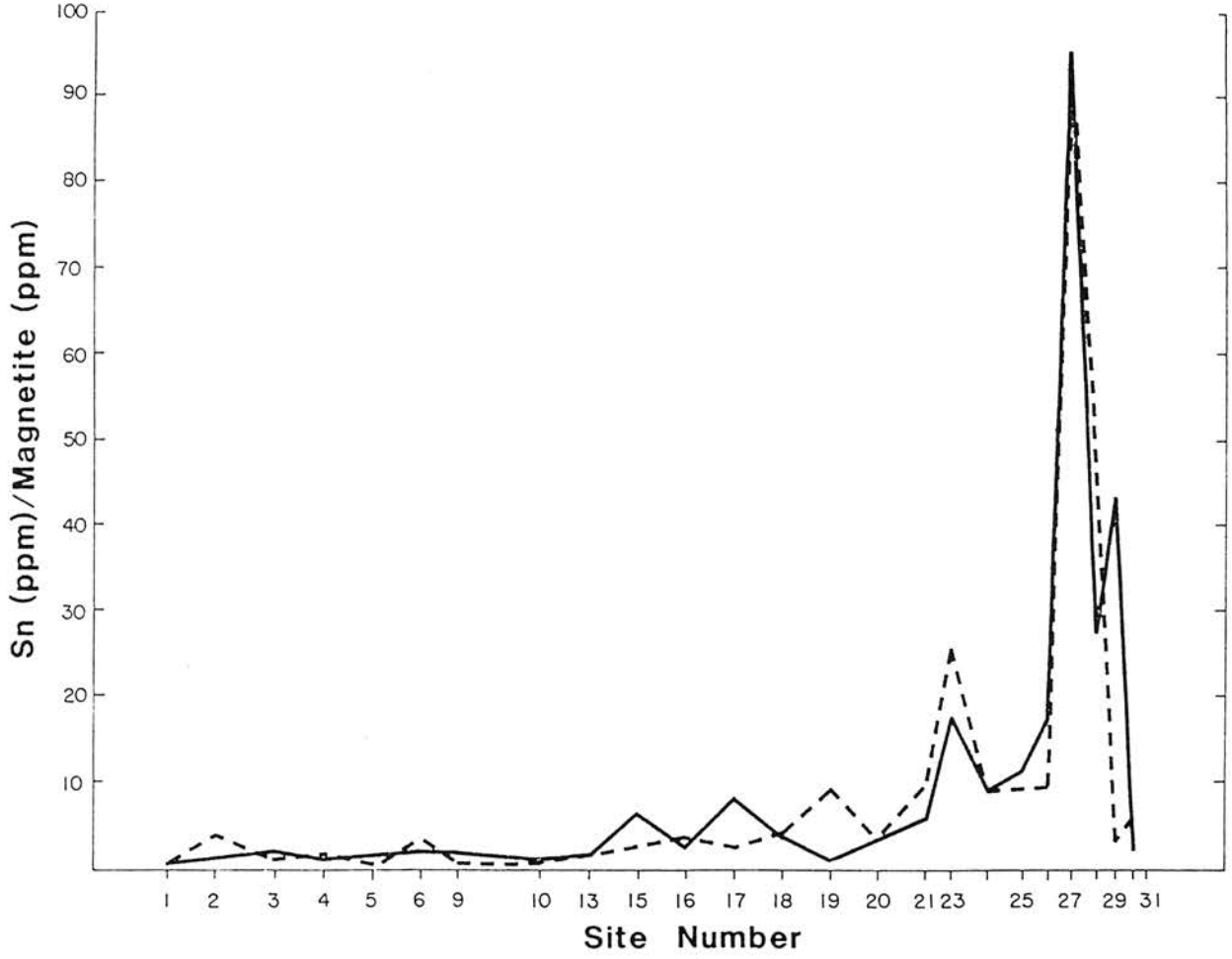

Fig. 38 Sn/magnetite ratios for the Sungei Petai, minus 65 + 100 -mesh sediment. Solid line high energy environment, dotted line low energy environment.

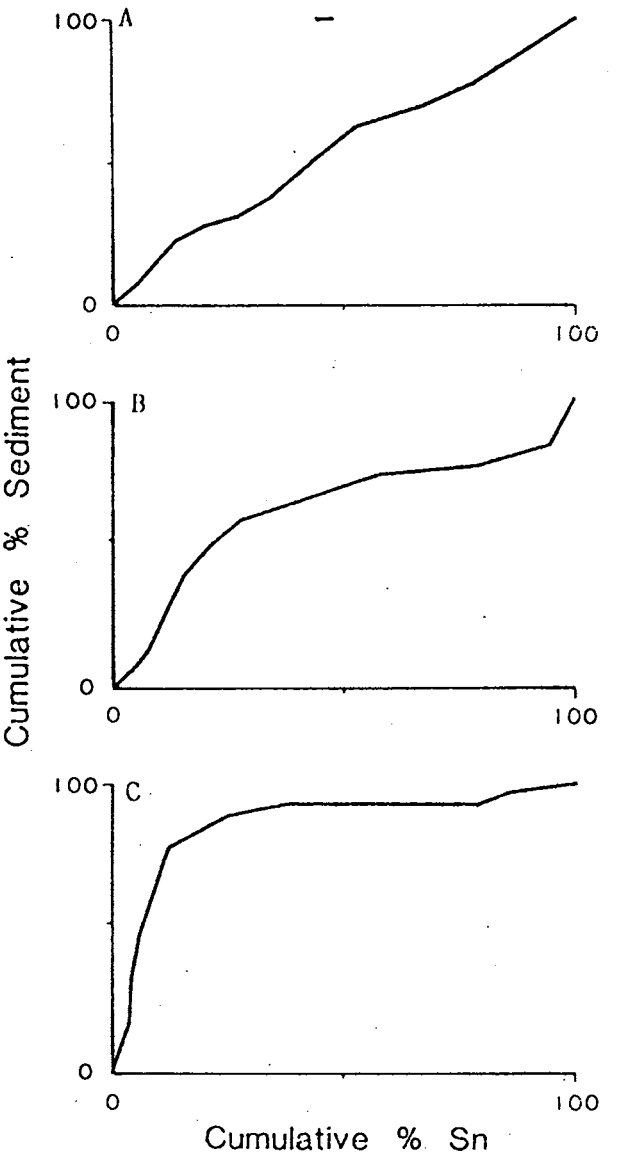

Fig. 39 Cumulative curves for sediment and tin. From Gladwell (1981).

A. Linear curve due to primary mineralization.
B. Sigmoidal curve caused by cassiterite accumulation.
C. Plateau curve typical of background localities.

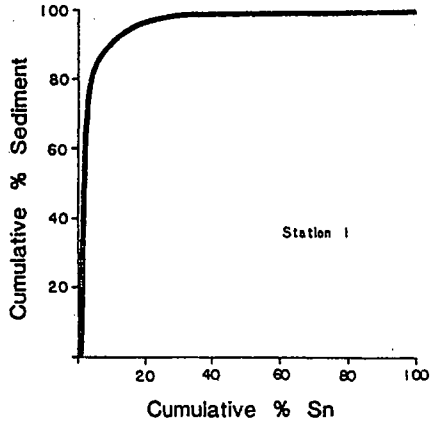

Fig. 40 Cumulative curve for Sn and sediment, high energy environment, Sungei Petai, Station 1.

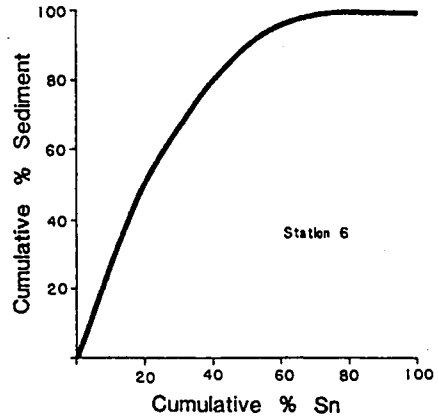

Fig. 41 Cumulative curve for Sn and sediment, high energy environment, Sungei Petai, Station 6.

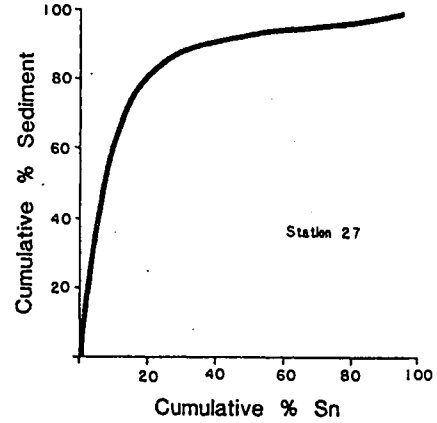

Fig. 42 Cumulative curve for Sn and sediment, high energy environment, Sungei Petai, Station 27.

With no theoretical prediction available for hydraulic equivalence of light and heavy mineral grains under real conditions, size fraction data from Sungei Petai have been used to derive an empirical relationship. By definition, and HEC is unaffected by changing hydraulic conditions but will reflect anomaly dilution thereby optimizing the variance ratio (F) for among-versus within-site variance. On this basis, all possible values of HECs were calculated for size fractions between minus 270 and minus 28+35 mesh, and the corresponding F values obtained (Table 11). Results show several interesting features:

(1) Using Miesch's criteria (Garrett, 1983) that V_m (i.e., F-1) should be at least three for regional patterns to be significant, only the minus 270- and minus 65+100-mesh fractions give satisfactory results in the original data.

(2) For size fractions up to minus 65+100 mesh, the maximum F values is obtained when the minus 65+100-mesh fraction is used for calculation of the HEC. F values systematically decrease for HECs calculated on grain sizes finer or coarser than minus 65+100 mesh.

(3) F values decrease going down the columns; for example, in the minus 65+100-mesh column, F decreases from 17.1 for the minus 270-mesh fraction to 5.6 for minus 150+100 mesh.

(4) For grain sizes coarser than minus 65+100 mesh, F values for the HECs are similar to those for the original size fraction.

These results are initially somewhat surprising in so far as they indicate that the minus 65+100-mesh fraction is the optimum size range for calculations of HECs for all finer size fractions. However, this is qualitatively consistent with calculations of the critical shear stresses required to initiate movement for a wide range of grain sizes of light and heavy minerals (Grigg and Rathbun, 1969). These calculations (Figure 43) suggest that, in addition to the much larger shear stress required for movement of heavy mineral grains, a relatively wide size range of fine heavy minerals can be set in motion by the change in critical shear stress required to initiate movement of a much narrower size range of light minerals.

Once selective transport of fine grains of light minerals is initiated, resistance of grains of the heavy mineral to further movement increases as a function of the ratio in diameter of the heavy grains to that of the remaining bedload material (Figure 44). Thus, once small grains of cassiterite become fixed in a bed of large quartz and fledspar grains, it will become extremely difficult for the flow to move them again. In the Sungei Petai, where the bulk of cassiterite occurs in the finest fractions of the sediment (Figures 33-35), this relationship may account for decreasing values of F associated with HECs in the minus 65+100-mesh fraction as the original grain size increases.

APPLICATION TO EXPLORATION

Studies on Bujang Melaka have shown that in hilly or mountainous terrain hydraulic conditions in streams are capable of selectively transporting grains of light minerals and accumulating cassiterite in the remaining bedload sediments. In effect, the action of the stream is similar to that of a sluice or palung. However, accumulation of cassiterite is very

TABLE 10
SN CONTENT OF BANK SAMPLES, SUNGEI PETAI

Location	Geometric mean (ppm)	Range (ppm)
Stations 25-30	245	25-2455
Stations 4-10	65	31-135

TABLE 11
F VALUES OF LOGARITHMIC BETWEEN/WITHIN SITE VARIANCES COMPUTED FOR ALL POSSIBLE HYDRAULIC EQUIVALENCES OF SN, SUNGEI PETAI (N=29)

Original size fraction	Hydraulic equivalent size fraction							
	-270	+270 / -200	+200 / -150	+150 / -100	+100 / -65	+65 / -48	+48 / -35	+35 / -28
270	4.7	4.2	5.0	10.2	17.1	8.7	9.4	2.7
+270-200		3.7	3.8	8.0	12.7	7.9	7.8	2.9
+200-150			1.8	3.0	5.4	4.6	4.4	2.3
+150-100				3.1	5.6	4.9	5.3	2.9
+100-65					4.7	4.0	4.7	4.0
+65-48						3.5	3.7	3.0
+48-35							3.3	2.3
+35-28								2.5

dF = 28/29 $F_{.05} = 1.84$ $f_{.01} = 2.39$

dependent on the local hydraulic environment, which increases sampling variability and prevents the regular downstream dilution and decay that are expected of a sediment anomaly away from its source (Rose *et al.*, 1979). As a result it becomes extremely difficult to define targets for follow-up exploration. Under these circumstances several approaches to improving data interpretation deservel consideration:

Sampling

Rapid changes in texture of bedload sediments, ranging from fine- and medium-grained sands to coarse sands and gravels are good indicators of variable hydraulic conditions and the possibility of variable accumulations of heavy minerals. The influence of this on sampling variability can be minimized by sampling sediments having similar textures as consistently as possible. If relatively low energy environments are sampled, both sampling variability and

the length of anomalous dispersion trains will be reduced. Conversely, sampling high energy environments will give longer but very erratic dispersion patterns (e.g., Figures 18 and 25-30).

Size fraction and sampling preparation

Tin content of all size fractions of the sediments is influenced by local hydraulic conditions. However, the difference in Sn concentrations for high and low energy environments is greatest for coarse size fractions and becomes insignificant below 200 mesh. For the Sungei Petai, Sn content of minus 80-mesh material is very erratic (Figure 18) reflecting its relatively coarse character. Nevertheless, except as noted below, there would not appear to be any advantage to collection and analysis of any other size fraction(s). In so far as sampling variability of minus 80-mesh material is much greater than analytical variability, there would be no benefit to grinding samples prior to their analysis by the methods employed in this study.

Where Sn is an element of particular interest, analysis of the finer (minus 200 mesh) fractions of the sediments might be of benefit by virtue of the relatively consistent accumulation of fine-grained cassiterite independent of local hydraulic conditions (Table 7; Figures 31-32). This results in enhanced, but relatively uniform, Sn concentrations extending a considerable distance from their source and might, therefore, be of particular value in low density reconnaissance surveys. This possibility requires further study and comparison to data obtained from low density surveys using heavy minerals concentrates. An additional advantage to the use of the finer fractions would be reduced subsampling errors during sample preparation and analysis. An obvious disadvantage is the difficulty of obtaining sufficient fine-grained material from swift mountain streams—preliminary on-site screening would probably be required.

Data interpretation

Interpretation of Sn distribution patterns can be improved by (1) consideration of pathfinder elements; (2) use of Sn/magnetite ratios; and (3) calculation of hydraulic equivalent concentrations.

Pathfinders

If the primary Sn mineralization is accompanied by pathfinder elements that are not transported in drainage sediments as heavy minerals, these can provide better anomaly contrast and more reliable identification of the source. At Ulu Petai this is illustrated by As, Cu, Pb and Zn (Figures 20-23), all of which are present in the primary mineralization as sulphides that will decompose during weathering. Useful supplementary information can be obtained by rapid mineralogical examination of heavy mineral concentrates for tourmaline or other minerals associated with the primary source.

Sn/magnetite ratios (Figure 38)

Providing magnetite is not associated with the primary tin mineralization (as it is in many skarn deposits) and supply of magnetite to streams within the survey area is relatively uniform, the similarity in hydraulic behaviour of Sn and magnetite can be used both to reduce

sampling variability caused by hydraulic effects and to distinguish hydraulic accumulations from near source anomalies. Further work is required to extend the findings of this study to a wider range of environments.

Hydraulic equivalent concentrations

Calculation of HECs provides no improvement in F values for fractions coarser than 100 mesh and would presumably be of little benefit with minus 80-mesh material where this consists predominantly, as in the Sungei Petai, of relatively coarse sand. However, when HECs are calculated for fine sand (minus 200+270 mesh) and silt (minus 270 mesh) fractions, F values are greatly improved. This is reflected in figure 45 by eliminetion of enhanced Sn values resulting from selective accumulation of cassiterite below Station 19 and by the correspondingly better definition of the anomaly source at Ulu Petai. The resulting dispersion pattern is very similar to that for the pathfinder elements (Figures 20-23). On this basis, calculation of HECs appear to have sufficient promise to warrant further study: both to confirm present findings and determine if they can be extended to a wider range of hydraulic conditions.

Heavy mineral concentrates

No attempt has been made in this study to make a detailed comparison of the relative merits of heavy mineral concentrates and routine geochemical prospecting methods for Sn. For Bujang Melaka both approaches appear to provide comparable, regionally anomalous, but erratic, data. It is, however, recommended that to retain the benefit of physically removing the influence of barren light minerals on Sn concentrations (and thereby reducing hydraulic effects), analyses of heavy mineral concentrates should be expressed directly as Sn content of the concentrate. This differs from the procedure usually used in evaluation for mining purposes when results are expressed in relation to a specified volume of ground.

CONCLUSIONS

Dispersion of Sn, as cassiterite, in mountain streams is strongly influenced by local hydraulic conditions that result in its concentration in high, compared to low, energy environments. This effect results in considerable local variability in Sn content of sediments and disrupts the systematic decay of sediment geochemical anomalies downstream from their source. Interpretation of Sn content of drainage sediments can therefore be difficult or even misleading. These problems can be overcome by (1) using pathfinder elements that are not dispersed as heavy minerals (e.g., As, Cu, Pb, Zn); (2) utilizing the Sn/magnetite ratio; or (3) plotting hydraulic equivalence values of Sn. In addition it is suggested that use of fine fractions (minus 200 mesh) of sediments might be beneficial for low density, regional reconnaissance surveys.

ACKNOWLEDGEMENTS

This study was undertaken as a joint project between the Southeast Asia Tin Research and Development (SEATRAD) Centre and the Geological Survey of Malaysia, with assistance from the United Nations Development Programme administered through the Economic and Social Commission for Asia and the Pacific.

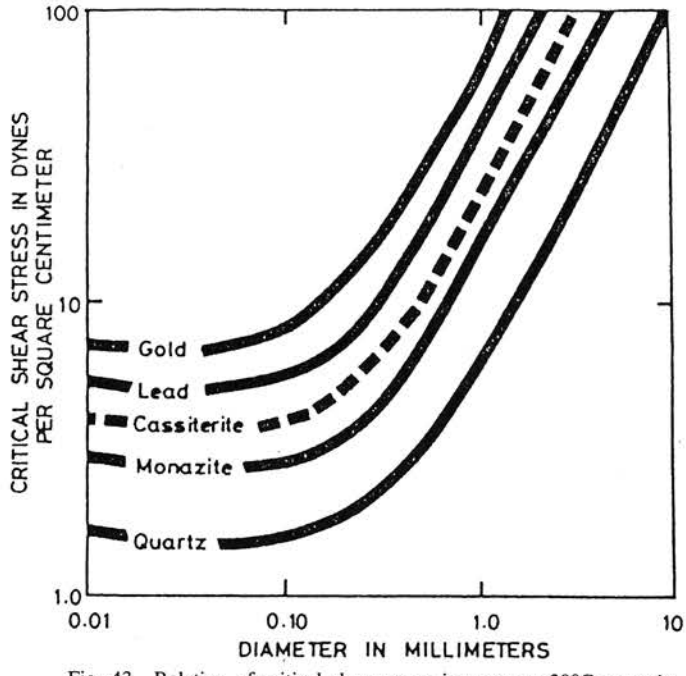

Fig. 43 Relation of critical shear stress in water at 20°C to grain diameter for minerals having different specific gravities. Modified from Grigg and Rathbun (1969) by interpolation of cassiterite line.

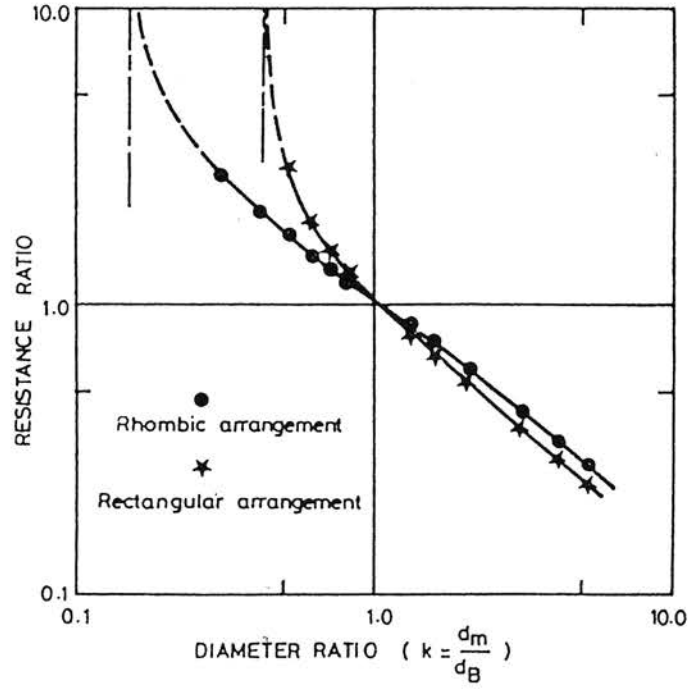

Fig. 44 Resistance of a particle to motion as a function of the ratio of its size (dm) to the size (dB) of the bed material. From Brandy and Jobson (1973).

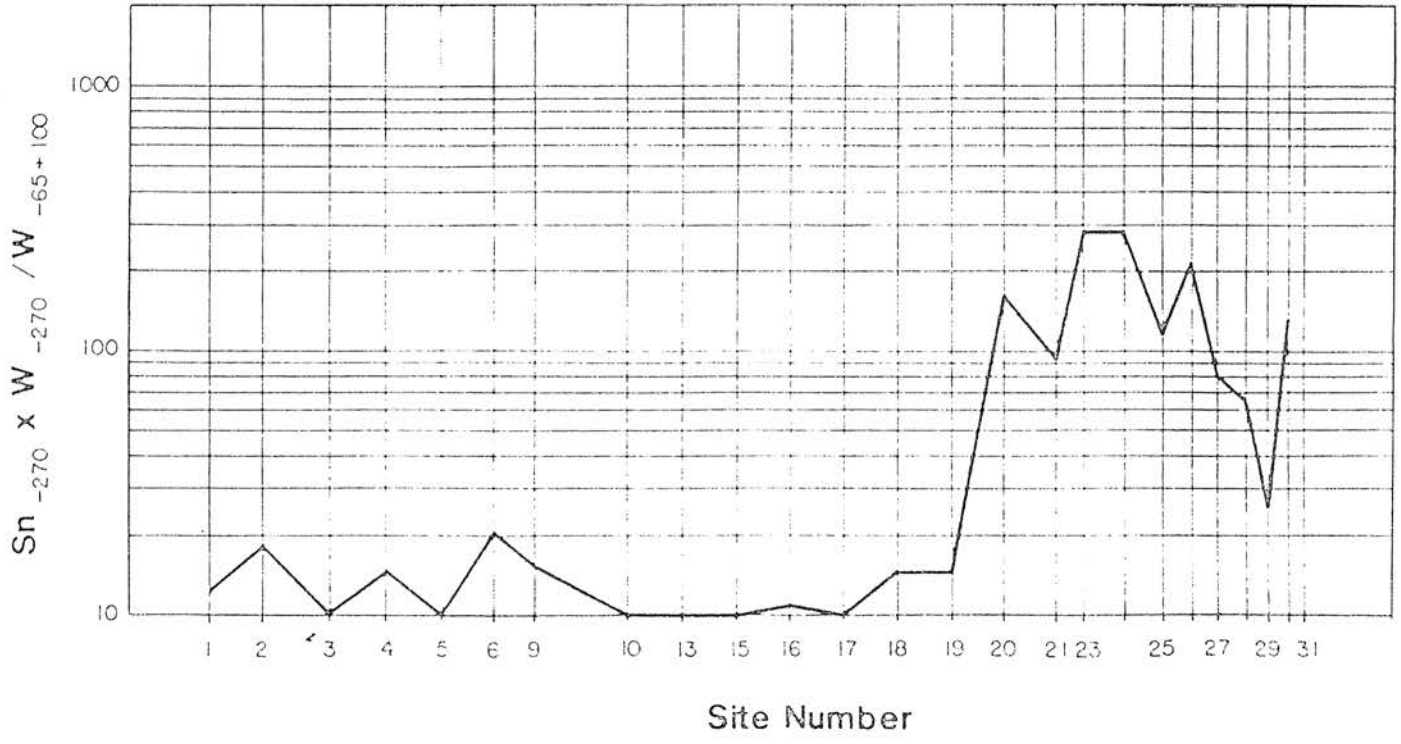

Fig. 45 Hydraulic equivalent concentration of minus 270-mesh tin in 65 + 100 -mesh fraction. Compare to Figure 32.

REFERENCES

BIGNELL, J.D. and SNELLING, N.J. 1977. Geochronology of Malayan granites. *Institute of Geological Sciences Overseas Geology and Mineral Resources Number 47*. HMSO, 70 pp.

BRADY, L.L. and JOBSON, H.E. 1973. An experimental study of heavy-mineral segregation under alluvial-flow conditions. *U.S. Geol. Surv. Prof. Paper 562-k*, 38 pp.

CHAND, F. 1981. A Manual of Geochemical Exploration Methods. *Geological Survey of Malaysia, Special Paper 3*.

FLETCHER, W.K. 1981. *Analytical Methods in Geochemical Prospecting*. Elsevier, 255 pp.

GARRETT, R.G. 1983. Sampling Methodology. *In* R.J. Howarth (Editor) *Statistics and Data Analysis in Geochemical Prospecting*. Elsevier, 83-107.

GLADWELL, D.R. 1981. *Research into geochemical exploration techniques for stanniferous mineralisation*. Unpub. Ph.D. thesis, Univ. of London, 283 pp.

GRIGG, N.S. and RATHBUN, R.E. 1969. Hydraulic equivalence of minerals with a consideration of the re-entrainment process. *U.S. Geol. Surv. Prof. Paper 650-B*, 77-80.

HAND, B.M. 1976. Differentiation of beach and dune sands using settling velocities of light and heavy minerals. *Journ. Sed. Pet. 37*, 514-520.

HOSKING, K.F.G., NAIK, S.M., BURN, R.E. and ONG, P. 1962. A study of the distribution of tin, tungsten, arsenic and copper in the sediments and of the total heavy metals in the water of the Menalhyl River, Mid Cornwall. *Cam. Sch. Min. Mag.* 62, 49-59.

INGHAM, F.T. and BRADFORD, E.F. 1960. The Geology and Mineral Resources of the Kinta Valley, Perak. *Federation of Malaya Geological Survey, District Memoir 9*, 347 pp.

KAEWBAIDHOON S. 1961. *Geochemical dispersion of tin in soils and stream sediments in Malaya*. Unpub. M.Sc. thesis, Univ. of London, 205 p.

LOWRIGHT, R., WILLIAMS, E.G. and DACHILE, F. 1972. An analysis of factors controlling deviations in hydraulic equivalence in some modern stands, *Journ. Sed. Pet., 42*, 635-645.

MCQUIVEY, R.S. and KEEFER, T.N. 1969. The relation of turbulence to deposition of magnetite over ripples. *U.S. Geol. Surv. Prof. Paper 650D*, 244-247.

RILEY, G.C. 1968. A description of various facets of the geology of a cassiterite-sulphide deposit at Ulu Petai, Bujang Melaka, Perak, Malaysia. *Unpub. Report, Geological Survey of Malaysia*, 19 pp.

RITTENHOUSE, G. 1943. Transportation and deposition of heavy minerals. *Bull. Geol. Soc. Amm., 54*, 1725-1780.

ROSE, A.W., HAWKES, H.E. and WEBB, J.S. 1979. *Geochemistry in Mineral Exploration, 2nd Ed.*, Academic Press, 657 pp.

SINCLAIR, A.J. 1976. Applications of Probability Graphs in Mineral Exploration. *Association of Exploration Geochemists, Rexdale, Ont.*, 95 pp.

SLEATH, A. and FLETCHER, W.K. 1982. Geochemical dispersion in a glacial meltwater stream, Purcell Mountains, B.C. In *Proceedings of Symposium on Prospecting in Glaciated Terrain*, Inst. Min. Metal. London.

SLINGERLAND, R.L. 1977. The effect of entrainment on the hydraulic equivalence relationship of light and heavy minerals in sands. *Journ. Sed. Pet. 47*, 753-770.

TOURTELOT, H.A. 1968. Hydraulic equivalence of grains of quartz and heavier minerals, and implications for the study of placers. *U.S. Geol. Surv. Prof. Paper 594-F*, 13 pp.

ZANTOP, H. and NESPEREIRA, J. 1979. Heavy-mineral panning techniques in exploration for tin and tungsten in northwestern Spain. In J.R. Watterson and P.K. Theobald(eds.) *Geochemical Exploration 1978*, Association of Exploration Geochemists, Rexdale, Ont., 329-336.

Manuscript received 11th May 1985